Universidad de Concepción
Dirección de Postgrado
Facultad de Ingeniería Agrícola
Programa de Magíster en Ingeniería Agrícola con menciones en Agroindustrias, Mecanización y Energía, y Recursos Hídricos

PRONÓSTICO DE LA EVAPOTRANSPIRACIÓN DE REFERENCIA EN EL CLIMA MEDITERRÁNEO DE LA ZONA CENTRAL DE CHILE USANDO LA ECUACIÓN DE PENMAN-MONTEITH ESTANDARIZADA DE LA ASCE, LA ECUACIÓN DE HARGREAVES-SAMANI Y LAS PREDICCIONES METEOROLÓGICAS DEL MODELO GLOBAL FORECAST SYSTEM

FORECASTING REFERENCE EVAPOTRANSPIRATION IN THE MEDITERRANEAN CLIMATE OF CENTRAL CHILE USING THE ASCE STANDARDIZED PENMAN-MONTEITH EQUATION, THE HARGREAVES-SAMANI EQUATION, AND WEATHER PREDICTIONS FROM THE GLOBAL FORECAST SYSTEM MODEL

Tesis para optar al grado de Magíster en Ingeniería Agrícola con Mención en Recursos Hídricos

FERNANDO PATRICIO GÓMEZ DÍAZ
2024
Chillán, Chile

Profesor Guía: Dr. Octavio Lagos Roa
Depto. de Recursos Hídricos
Facultad de Ingeniería Agrícola
Universidad de Concepción

Esta tesis ha sido realizada en el Departamento de Recursos Hídricos de la Facultad de Ingeniería Agrícola, Universidad de Concepción.

Profesor Guía

Dr. Octavio Lagos Roa
Facultad de Ingeniería Agrícola
Universidad de Concepción

Comisión Evaluadora:

Dra. Pilar Gil Montenegro
Facultad de Agronomía y Sistemas Naturales
Pontificia Universidad Católica de Chile

Dr. Jorge Jara Ramírez
Facultad de Ingeniería Agrícola
Universidad de Concepción

Director de Programa

Dr. Pedro Melín Marín
Facultad de Ingeniería Agrícola
Universidad de Concepción

ACKNOWLEDGMENTS

Firstly, I would like to express my gratitude to Dr. Octavio Lagos, the guiding professor in this thesis, for his support both academically and personally, and for his valuable contribution to the development of this research. I also want to convey my appreciation to Professors Dr. Pilar Gil, Dr. Jorge Jara, and Dr. Daniele Zaccaria, who provided essential guidance and significantly contributed to the improvement of this work. Additionally, I extend my thanks to the professors and classmates at the Facultad de Ingeniería Agrícola of the Universidad Concepción, in Chillán, for their support and enriching academic environment throughout my studies. Finally, I thank my family for their unwavering support throughout this process.

CONTENTS

LIST OF TABLES

LIST OF FIGURES

RESUMEN

La estimación precisa de la evapotranspiración de cultivo (ET_c) es esencial para la planificación efectiva de los recursos hídricos agrícolas y, para determinar ET_c, es común multiplicar la evapotranspiración de referencia (ET_{ref}) por un coeficiente de cultivo apropiado (K_c). Pronosticar ET_{ref} podría ser particularmente beneficioso para la programación del riego. En este trabajo, se evaluaron las predicciones diarias y acumuladas (7 días) de ET_{ref} obtenidas con los modelos de Penman-Monteith (PM) y Hargreaves-Samani (HS), y usando el Global Forecast System (GFS). Se utilizaron cuatro estaciones meteorológicas ubicadas en el la Zona Central de Chile durante el periodo 2020 a 2022. Los resultados se compararon con la ET_{ref} calculada con la ecuación de PM de la ASCE (American Society of Civil Engineers) a partir de valores diarios medidos de: radiación solar, temperatura del aire, humedad relativa y velocidad del viento. Los mejores resultados se obtuvieron utilizando la ecuación de HS; para todas las estaciones meteorológicas, los indicadores estadísticos para las predicciones diarias de ET_{ref} se encuentran dentro de los siguientes rangos: $Accuracy$ (definido como el porcentaje de predicciones diarias de ET_{ref} con un error absoluto dentro de $1\,mm, d^{-1}$) varía entre $72.8\,\%$ y $91.8\,\%$; el error cuadrático medio ($RMSE$) oscila entre $0.59\,mm\,d^{-1}$ y $0.98\,mm\,d^{-1}$; el error cuadrático medio normalizado ($NRMSE$) está entre $16.1\,\%$ y $24.1\,\%$; el error de sesgo medio (MBE) está entre $0.10\,mm\,d^{-1}$ y $0.36\,mm\,d^{-1}$; y el error de sesgo medio normalizado ($NMBE$) varía del $2.5\,\%$ al $8.3\,\%$. Por otro lado, los indicadores para las predicciones acumuladas de ET_{ref} en 7 días caen dentro de los siguientes rangos: $RMSE$ de $2.86\,mm$ a $5.08\,mm$; $NRMSE$ de $11.0\,\%$ a $16.3\,\%$; MBE de $0.66\,mm$

a $2.57\,mm$; y $NMBE$ de $2.4\,\%$ a $8.3\,\%$. Estos resultados sugieren que los valores de ET_{ref} de HS pronosticados a partir de las predicciones de temperatura del GFS podrían ser efectivos para prever la demanda hídrica a corto plazo y mejorar la precisión de la programación y gestión del riego en el centro de Chile.

ABSTRACT

Accurate estimation of crop evapotranspiration (ET_c) is essential for effective agricultural water resource planning and to determine ET_c it is common multiplying the reference evapotranspiration (ET_{ref}) by an appropriate crop coefficient (K_c). Forecasting ET_{ref} could be particularly beneficial for irrigation scheduling. In this work, daily and cumulative (7 days) ET_{ref} predictions were evaluated with the Penman-Monteith (PM) and the Hargreaves-Samani (HS) models using the Global Forecast System (GFS). Four weather stations located in Central Chile during 2020 to 2022 were used. Results were compared with ET_{ref} calculated with the ASCE (American Society of Civil Engineers) PM equation from measured daily values of: solar radiation, air temperature, relative humidity and wind speed. The best results were obtained using the HS equation, for all weather stations, the statistical indicators for daily ET_{ref} predictions fall within the following ranges: $Accuracy$ (defined as the percentage of daily ET_{ref} predictions with an absolute error within $1\,mm\,d^{-1}$) varies between $72.8\,\%$ and $91.8\,\%$; the root mean square error ($RMSE$) ranges from $0.59\,mm\,d^{-1}$ to $0.98\,mm\,d^{-1}$; the normalized root mean square error ($NRMSE$) is between $16.1\,\%$ and $24.1\,\%$; the mean bias error (MBE) is between $0.10\,mm\,d^{-1}$ and $0.36\,mm\,d^{-1}$; and the normalized mean bias error ($NMBE$) varies from $2.5\,\%$ to $8.3\,\%$. On the other hand, the indicators for the 7-day cumulative ET_{ref} forecasts fall within the following ranges: $RMSE$ from $2.86\,mm$ to $5.08\,mm$; $NRMSE$ from $11.0\,\%$ to $16.3\,\%$; MBE from $0.66\,mm$ to $2.57\,mm$; and $NMBE$ from $2.4\,\%$ to $8.3\,\%$. These results suggest that HS ET_{ref} values predicted from GFS temperature forecasts could be effective for foreseeing near-future water demand and enhancing the accuracy of irrigation scheduling and management in

Central Chile.

CHAPTER 1

INTRODUCCIÓN

1.1 Pronóstico de la evapotranspiración

En el sistema continuo suelo-planta-atmósfera, la evapotranspiración (ET) representa el proceso integrado donde el agua líquida se transforma en vapor de agua, involucrando tanto la evaporación desde la superficie del suelo como la transpiración de las plantas (e.g., Allen et al. 1998; Allen et al. 2005; Reichardt y Timm 2020). La ET juega un papel crucial en el ciclo hidrológico y tiene una influencia directa en la gestión de recursos hídricos para la agricultura. En el caso de un cultivo típico, la evaporación ocurre principalmente a través de la superficie del suelo. La transpiración, por otro lado, implica la vaporización y remoción de agua líquida de los tejidos de las plantas.

Dado que la evaporación y la transpiración de un cultivo ocurren simultáneamente, no existe una forma sencilla de diferenciarlas. Típicamente, durante la fase inicial del crecimiento de la planta, casi el 100 % de ET ocurre en forma de evaporación, mientras que, a medida que la cobertura vegetal se completa, más del 90 % de ET ocurre a través de la transpiración.

Factores meteorológicos como la radiación solar, la temperatura del aire, la humedad atmosférica y la velocidad del viento influyen en el proceso de ET. La tasa de ET también se ve influenciada por el contenido de agua en el suelo, la conductividad y la salinidad, así como por las características específicas del cultivo (tipo, etapa de desarrollo fenológico y

cobertura). La ET se expresa usualmente en milímetros por unidad de tiempo, como por ejemplo $mm\ h^{-1}$, $mm\ d^{-1}$ o $mm\ mes^{-1}$.

Para estimar la ET, se pueden utilizar mediciones de campo o modelos basados en variables meteorológicas. La determinación experimental de ET en campo requiere de equipos específicos y mediciones precisas de parámetros físicos, lo que hace que estos métodos se reserven generalmente para la investigación científica. Por otro lado, la estimación de ET a partir de datos meteorológicos es más accesible, y existen modelos como Penman-Monteith (PM) y Hargreaves-Samani (HS) para este propósito.

En esta investigación, es de interés el ampliamente aceptado modelo de PM. Este incorpora una ecuación basada en principios físicos, y que también considera aspectos fisiológicos de la planta. Las variables meteorológicas utilizadas en esta ecuación son la radiación solar, la temperatura del aire, la humedad atmosférica y la velocidad del viento. Los aspectos relacionados con el cultivo en la ecuación PM incluyen resistencias superficiales y aerodinámicas, y el albedo. Dado que diferentes tipos de plantas presentan variaciones en estas características, es útil definir un cultivo estándar, cuya ET se conoce como evapotranspiración de referencia (ET_{ref}), y se puede utilizar para determinar la ET de otros cultivos, que se denomina evapotranspiración del cultivo (ET_c).

La relación entre ET_c y ET_{ref} es dada por la expresión $ET_c = K_c \times ET_{ref}$, donde la constante de proporcionalidad K_c es el coeficiente de cultivo. Esta cantidad caracteriza cada cultivo y se puede determinar experimentalmente. Teniendo en cuenta que las plantas cambian durante su crecimiento, se deben considerar diferentes valores de K_c correspondientes a las distintas etapas desde la siembra hasta la cosecha.

El documento *The ASCE Standardized Reference Evapotranspiration Equation* (Allen 2005) presenta un método para calcular ET_{ref} (diaria u horaria) dentro de un marco de aplicación estandarizado, que unifica el uso de la ecuación PM. El procedimiento de cálculo de ET_{ref} de ASCE se define para dos cultivos de referencia: uno corto, con una altura aproximada de 12 cm (similar a una empastada recortada, de temporada fría), y

uno alto, con una altura aproximada de 50 cm (similar a alfalfa de cobertura completa).

Considerando que no siempre es factible obtener un conjunto completo y confiable de datos para las cuatro variables meteorológicas en el método PM para ET_{ref} (radiación solar, temperatura del aire, humedad atmosférica y velocidad del viento), es usual utilizar modelos simplificados. Un enfoque ampliamente utilizado es el modelo HS (Hargreaves y Samani 1985; Hargreaves y Allen 2003), basado únicamente en las temperaturas máximas y mínimas, junto con coeficientes de ajuste. Este modelo ofrece una solución práctica cuando no se dispone de conjuntos de datos completos, y aún así proporciona estimaciones razonablemente precisas en diferentes climas.

Independientemente del modelo considerado, una estimación precisa de ET_{ref} es crucial para una gestión eficiente del riego, permitiendo ajustar el volumen y la frecuencia de riego, para promover tanto altos rendimientos como calidad óptima, mientras se asegura un uso racional de los recursos hídricos y energéticos. La programación del riego agrícola típicamente se basa en estimaciones casi en tiempo real de ET_{ref} a través de cálculos que utilizan datos meteorológicos medidos casi en tiempo real (es decir, datos de hoy, ayer, la semana pasada). Aunque en la práctica este método es útil, es evidente que buenos pronósticos de ET_{ref} podrían ser más ventajosos. Por un lado, se podría lograr así una mayor precisión y exactitud en la estimación de las necesidades hídricas del cultivo. Por otro lado, se podría contar con más información a futura, dependiendo del número de días en el horizonte del pronóstico.

Dependiendo del enfoque elegido y de los datos de entrada, los métodos de pronóstico para ET_{ref} se pueden clasificar como directos o indirectos (Liu et al. 2020; Yang et al. 2016). Los métodos directos principales son el método de series temporales y, el de las redes neuronales artificiales, ambos basados en datos meteorológicos históricos y resultando más adecuados para predicciones de ET_{ref} a mediano o largo plazo (Yang et al. 2016). En contraste, los métodos indirectos incorporan pronósticos de variables meteorológicas en un modelo de ET, como el de PM (Allen et al. 1998; Allen et al. 2005)

o el de HS (Hargreaves y Samani 1985). Estos enfoques pueden ser particularmente ventajosos para pronósticos diarios de ET_{ref} (Yang et al. 2016).

En esta tesis, el enfoque se centra en el segundo método. Artículos científicos publicados en los últimos años siguiendo este método incluyen, por ejemplo, Hamouda et al. (2022), Liu et al. (2020), Luo et al. (2014), Perera et al. (2014), Yang et al. (2016), y Zhang et al. (2022). En este marco, los pronósticos meteorológicos suelen ser proporcionados por fuentes externas (que pueden ser agencias nacionales o plataformas científicas, de alcance local o global), y estas predicciones se evalúan luego en un modelo de ET para obtener pronósticos de ET_{ref}. Aquí se asume que existe buena calidad en los pronósticos de las variables meteorológicas requeridas y una cantidad adecuada de datos, que a menudo es extensa.

El Global Forecast System 384-Hour Predicted Atmosphere Data, o GFS, es un modelo que proporciona pronósticos para 384 horas (16 días) de 9 variables meteorológicas, incluidas las cuatro consideradas en el modelo PM. El GFS, que combina modelos atmosféricos, oceánicos, de suelo/terreno y de hielo marino, es interesante porque sus pronósticos meteorológicos para cualquier ubicación en el mundo son de acceso público y se pueden descargar utilizando la plataforma Google Earth Engine (GEE). Este modelo de predicción ha sido utilizado en diversas áreas de investigación, como la predicción de la velocidad del viento (Zhao et al. 2016), la precipitación (Yue et al. 2022), las propiedades de las nubes (Yoo y Li 2012), la migración de aves (Van Doren y Horton 2018), la intensidad de huracanes (Xue et al. 2013), el transporte y dispersión de contaminantes atmosféricos (Rolph et al. 2017), y también en la estimación de ET (Tian y Martinez 2012a, 2012b).

Durante la última década, se han publicado numerosos artículos científicos sobre el pronóstico de ET_{ref}. Sin embargo, prácticamente no hay información sobre el pronóstico de ET_{ref} en Chile (excepto por el artículo de Silva et al. 2010, donde los autores emplean un enfoque de pronóstico diferente). Esto motivó la presente investigación, que se enfoca en la evaluación del pronóstico diario y acumulativo de ET_{ref} en el clima mediterráneo de

la zona central de Chile, donde se realiza la mayor parte de la agricultura de riego del país. Para este propósito, se utilizará la ecuación estandarizada de PM de ASCE y la ecuación de HS, junto con datos meteorológicos proporcionados por el modelo de predicción GFS en la plataforma GEE.

1.2 Hipótesis y objetivos

En relación a lo expresado anteriormente, se plantean las hipótesis y objetivos de esta investigación:

Hipótesis (H): Basándose en pronósticos de las variables meteorológicas temperatura del aire, velocidad del viento, radiación, y/o humedad relativa, realizados por el modelo GFS en GEE, es posible obtener predicciones razonables de ET_{ref} diaria y acumulativa dentro del rango de 1-7 días para la temporada de riego en el clima mediterráneo de la zona central de Chile.

Aquí, se entiende por predicciones razonables a aquellas asociadas con un índice de $Exactitud$ de $\approx 80\,\%$ en ET_{ref} diaria. La $Exactitud$ se define en esta tesis como el porcentaje de predicciones de ET_{ref} con un error absoluto menor o igual a $1\ mm\ d^{-1}$ (cabe señalar que en Luo et al. 2014 y Zhang et al. 2022 el indicador $Exactitud$ se definió considerando un error absoluto de $1.5\,mm\,d^{-1}$, en lugar de $1\,mm\,d^{-1}$).

Objetivo General (OG): Evaluar los pronósticos diarios y acumulativos de ET_{ref} realizados con los modelos PM estandarizado de ASCE y HS, utilizando predicciones meteorológicas de GFS, dentro del rango de 1-7 días para cuatro estaciones meteorológicas de la red Agrometeorología situadas en el clima mediterráneo de la zona central de Chile, durante las temporadas de riego en el período de tres años 2020-2022.

Objetivos Específicos (OE):

OE1. Analizar la pertinencia de cuatro estaciones meteorológicas pertenecientes a

la red Agrometeorología en la zona central de Chile, con el fin de estimar ET_{ref} diaria utilizando la ecuación PM de ASCE.

OE2. Comparar los pronósticos meteorológicos de GFS necesarios para estimar ET_{ref} diaria, con los datos correspondientes obtenidos de las estaciones meteorológicas seleccionadas.

OE3. Evaluar los pronósticos diarios y acumulativos de ET_{ref} realizados con datos de GFS utilizando series temporales, gráficos 1:1 e indicadores estadísticos.

1.3 Artículo sobre el pronóstico diario y acumulativo de ET_{ref}

Las hipótesis y objetivos formulados permitieron desarrollar una investigación, que dio como resultado un manuscrito titulado *Forecasting Reference Evapotranspiration in the Mediterranean Climate of Central Chile using the ASCE Standardized Penman-Monteith Equation, the Hargreaves-Samani Equation, and Weather Predictions from the Global Forecast System Model*, el cual ya ha sido enviado para su publicación (julio de 2024).

Ese documento constituye el grueso de esta tesis, y se incorporará casi en su totalidad en el Capítulo 3. Es importante señalar que el resumen del manuscrito se ha incluido al principio de esta tesis (ver página xv), y la lista completa de referencias se puede encontrar al final (ver página 65), por lo tanto, ambas secciones no se incluyen en el Capítulo 3.

El artículo en el Capítulo 3 está estructurado de la siguiente manera: En la Sección 3.1 (Introducción), se presentan los antecedentes y el propósito de la investigación. En la Sección 3.2 (Materiales y Métodos), se seleccionan las estaciones meteorológicas incluidas en este estudio, se introducen la ecuación ET_{ref} PM estandarizada de ASCE y la ecuación HS, se revisan aspectos clave relacionados con la obtención de los datos meteorológicos pronosticados del GFS y observados, y se presentan los indicadores estadísticos utilizados para evaluar las predicciones de ET_{ref}. La Sección 3.3 (Resultados y Discusión) incluye la ejecución de pronósticos diarios y acumulativos de ET_{ref} utilizando

las predicciones de variables meteorológicas de GFS y, los métodos sugeridos por ASCE y el modelo HS. Estos pronósticos se evalúan posteriormente a través de análisis de series temporales, gráficos 1:1 e indicadores estadísticos. La Sección final 3.4 (Conclusiones) proporciona un resumen de los principales hallazgos de la investigación y observaciones finales.

Luego, directamente después del artículo en el Capítulo 3, se presentan las conclusiones finales de esta tesis, en español y en inglés, en los Capítulos 4 y 5, respectivamente.

CHAPTER 2

INTRODUCTION

2.1 Evapotranspiration forecasting

In a soil-plant-atmosphere continuum system, evapotranspiration (ET) represents the integrated process where liquid water undergoes transformation into water vapor, involving both soil surface evaporation and plant transpiration (e.g., Allen et al. 1998; Allen et al. 2005; Reichardt and Timm 2020). ET plays a crucial role in the hydrological cycle and exerts a direct influence on water resource management in agriculture. In the case of a typical crop, evaporation mainly occurs through the soil surface. Transpiration, on the other hand, involves the vaporization and removal of liquid water from plant tissues.

Since the evaporation and transpiration of a crop occur simultaneously, there is no simple way to distinguish between them. Typically, during the initial phase of plant growth, nearly 100 % of ET occurs in the form of evaporation, whereas, as the vegetative cover becomes complete, over 90 % of ET occurs through transpiration.

Meteorological factors such as solar radiation, air temperature, atmospheric humidity, and wind speed influence the ET process. The rate of ET is also influenced by the soil's water content, conductivity, and salinity, as well as the specific characteristics of the crop (type, phenological development stage, and coverage). ET is usually expressed in millimeters per unit of time, such as $mm\ h^{-1}$, $mm\ day^{-1}$, or $mm\ month^{-1}$.

To estimate ET, field measurements or models based on weather variables can be

used. Experimental determination of ET in the field requires specific equipment and precise measurements of physical parameters, making these methods typically reserved for scientific research. On the other hand, estimating ET from meteorological data is more accessible, and models such as Penman-Monteith (PM) and Hargreaves-Samani (HS) exist for this purpose.

In this research, the widely accepted PM ET model is of interest. It incorporates a physically based equation considering physiological aspects of the plant. The meteorological variables used in this equation are solar radiation, air temperature, atmospheric humidity, and wind speed. Crop-related aspects in the PM equation include surface and aerodynamic resistances and albedo. As different types of plants exhibit variations in these characteristics, defining a standard crop, with its ET known as reference evapotranspiration (ET_{ref}), is useful for determining ET for other crops, denoted as crop evapotranspiration (ET_c).

The relation between ET_c and ET_{ref} is given by the expression $ET_c = K_c \times ET_{ref}$, where the proportionality constant K_c is the crop coefficient. This quantity characterizes each crop and can be determined experimentally. Considering that plants change during their growth, different values of K_c corresponding to different stages from planting to harvest must be considered.

The document The ASCE Standardized Reference Evapotranspiration Equation (Allen 2005) presents a method for calculating ET_{ref} (daily or hourly) as a standardized application framework, unifying the use of the PM equation. The ASCE ET_{ref} calculation procedure is defined for two reference crops: a short one with an approximate height of 12 cm (similar to clipped, cold-season grass) and a tall one with an approximate height of 50 cm (similar to full-cover alfalfa).

Considering it is not always feasible to obtain a complete and reliable dataset for the four meteorological variables solar radiation, air temperature, atmospheric humidity, and wind speed in the ET_{ref} PM method, simpler frameworks are often preferred. One widely

used approach is the HS model (Hargreaves and Samani 1985; Hargreaves and Allen 2003), which relies solely on maximum and minimum temperatures along with adjustment coefficients. This model offers a practical solution when full datasets are not available, yet still provides reasonably accurate estimates across different climates.

Regardless of the model under consideration, an accurate estimation of ET_{ref} is crucial for efficient irrigation management, enabling the adjustment of the volume and frequency of irrigation to promote both high yields and optimal quality, all while ensuring a rational use of water and energy resources. Agricultural irrigation scheduling typically relies on near-real-time estimations of ET_{ref} through calculations using weather data measured almost in real-time (i.e., data from today, yesterday, last week). While in practice this method is useful, it is evident that good ET_{ref} forecasts could be more advantageous. On the one hand, higher accuracy and precision in estimating crop water needs could be achieved. On the other hand, more future information could be available, depending on the number of days in the forecast horizon.

Depending on the chosen approach and input data, forecasting methods for ET_{ref} can be classified as either direct or indirect (Liu et al. 2020; Yang et al. 2016). Two primary direct methods include the time series method and artificial neural networks, both relying on historical meteorological data and proving more suitable for medium or long-term ET_{ref} predictions (Yang et al. 2016). In contrast, indirect methods incorporate weather variable forecasts into an ET model, such as the PM (Allen et al. 1998; Allen et al. 2005) or the HS (Hargreaves and Samani 1985). These approaches may be particularly advantageous for daily ET_{ref} forecasts (Yang et al. 2016).

In this thesis, the focus is on the second approach. Scientific articles published in recent years following this method include, for example, Hamouda et al. (2022), Liu et al. (2020), Luo et al. (2014), Perera et al. (2014), Yang et al. (2016), and Zhang et al. (2022). In this framework, weather forecasts are usually provided by external sources (which can be national agencies or scientific platforms, with local or global scope), and these predictions

are then evaluated in an ET model to obtain ET_{ref} forecasts. It is assumed here that there is good quality for the forecasts of the required meteorological variables and an adequate amount of data, which is often extensive.

The Global Forecast System 384-Hour Predicted Atmosphere Data, or GFS, is a model that provides forecasts for 384 hours (16 days) of 9 meteorological variables, including the four considered in the PM model. GFS, which combines atmospheric, ocean, land/soil, and sea ice models, is interesting because its meteorological forecasts for any location worldwide are publicly accessible and can be downloaded using the Google Earth Engine (GEE) platform. This prediction model has been used in various research areas, such as predicting wind speed (Zhao et al. 2016), precipitation (Yue et al. 2022), cloud properties (Yoo and Li 2012), bird migration (Van Doren and Horton 2018), hurricane intensity (Xue et al. 2013), atmospheric pollutant transport and dispersion (Rolph et al. 2017), and also in ET estimation (Tian and Martinez 2012a, 2012b).

Over the last decade, numerous scientific articles on the forecast of ET_{ref} have been published. However, there is practically no information on ET_{ref} forecasting in Chile (except for the paper by Silva et al. 2010, where the authors employ a different forecasting approach). This motivated the present research, which focuses on the evaluation of daily and cumulative ET_{ref} forecast in the Mediterranean climate of central zone of Chile, where most of the country's irrigated agriculture takes place. The ASCE standardized PM equation and the HS equation, together with meteorological data provided by the GFS prediction model on the GEE platform, will be used for this purpose.

2.2 Hypotheses and objectives

In relation to what is expressed above, the hypotheses and objectives of this research are outlined:

Hypothesis (H): Based on forecasts of meteorological variables air temperature, wind

speed, radiation, and/or relative humidity, performed by the GFS model in GEE, it is possible to obtain reasonable predictions of daily and cumulative ET_{ref} within the range 1-7 days for the irrigation season in the Mediterranean climate of central zone of Chile.

Here, reasonable predictions are understood to be those associated with an $Accuracy$ index of $\approx 80\ \%$ in daily ET_{ref}. $Accuracy$ is defined in this thesis as the percentage of ET_{ref} predictions having an absolute error less than or equal to $1\ mm\ d^{-1}$ (note that in Luo et al. 2014 and Zhang et al. 2022 the $Accuracy$ index was defined considering an absolute error of $1,5\ mm\ d^{-1}$, instead of $1\ mm\ d^{-1}$).

General Objective (GO): Evaluate daily and cumulative ET_{ref} forecasts conducted with the ASCE standardized PM and HS models, utilizing GFS weather predictions, within the range 1-7 days for four weather stations of the network Agrometeorologia situated in the Mediterranean climate of central zone of Chile, throughout the irrigation seasons in the three-year period 2020-2022.

Specific Objectives (EO):

EO1. Analyze the pertinence of four meteorological stations belonging to the network Agrometeorología in the central zone of Chile, in order to estimate daily ET_{ref} using the ASCE PM equation.

EO2. Compare the GFS weather forecasts required to estimate daily ET_{ref}, with the corresponding data obtained from selected meteorological stations.

EO3. Evaluate daily and cumulative ET_{ref} forecasts conducted with GFS data using time series, 1:1 plots, and statistical indicators.

2.3 Paper on daily and cumulative ET_{ref} forecasting

The hypothesis and objectives outlined led to the development of a study, resulting in a manuscript titled *Forecasting Reference Evapotranspiration in the Mediterranean Climate*

of Central Chile using the ASCE Standardized Penman-Monteith Equation, the Hargreaves-Samani Equation, and Weather Predictions from the Global Forecast System Model, which has already been submitted for publication (July 2024).

That document constitutes the bulk of this thesis, and it will be incorporated nearly in its entirety into Chapter 3. It's worth noting that the abstract of the manuscript has been included at the beginning of this thesis (see page xv), and the comprehensive list of references can be found towards the end (see page 65), thus both sections are not included in Chapter 3.

The paper in Chapter 3 is structured as follows: In Section 3.1 (Introduction), antecedents and the research purpose are introduced. In Section 3.2 (Materials and Methods), the weather stations included in this study are selected, the ASCE standardized PM ET_{ref} equation and HS equation are introduced, key aspects related to obtaining GFS forecasted and observed meteorological data are reviewed, and the statistical indicators used to evaluate ET_{ref} predictions are presented. Section 3.3 (Results and Discussion) involves the execution of single-day and cumulative ET_{ref} forecasts using the GFS weather variable predictions and the methods suggested by the ASCE and the HS model. These forecasts are subsequently assessed through time series analysis, 1:1 plots, and statistical indicators. The final Section 3.4 (Conclusions) provides a summary of the primary research findings and concluding remarks.

Then, directly after the article in Chapter 3, the final conclusions of this thesis are presented, in Spanish and English, in Chapters 4 and 5, respectively.

CHAPTER 3

FORECASTING REFERENCE EVAPOTRANSPIRATION IN THE MEDITERRANEAN CLIMATE OF CENTRAL CHILE USING THE ASCE STANDARDIZED PENMAN-MONTEITH EQUATION, THE HARGREAVES-SAMANI EQUATION, AND WEATHER PREDICTIONS OF THE GLOBAL FORECAST SYSTEM MODEL

3.1 Introduction

In a soil-plant-atmosphere continuum system, evapotranspiration (ET) is the integrated process in which liquid water transforms into water vapor through both surface evaporation from wet soil and plant canopy transpiration (Allen et al. 1998; Allen et al. 2005; Reichardt and Timm 2020). ET is an important part of the hydrological cycle and it has a direct impact on water resource management in agriculture. Since experimental determination of crop evapotranspiration (ET_c) is costly and time consuming, it is common to compute crop water requirements from reference evapotranspiration (ET_{ref}), calculated from meteorological data, and using an appropriate crop coefficient (K_c), i.e., using the well known equation $ET_c = K_c \times ET_{ref}$.

In this context, a widely accepted approach to estimate ET_{ref} is the Penman-Monteith (PM) model (Allen et al. 1998; Allen et al. 2005; Reichardt and Timm 2020), which involves the use of four weather variables: air temperature, relative humidity, solar radiation and

wind speed. To establish a common and simplified method for ET_{ref} computation using the PM equation, in 2005, the American Society of Civil Engineers (ASCE) introduced its standardized ET_{ref} equation (Allen et al. 2005), which has been extensively used to determine ET_{ref}.

Since it is not always possible to have complete and reliable data sets of these four meteorological variables, simplified ET_{ref} computation procedures have been developed, such as the well-known Hargreaves-Samani (HS) model (Hargreaves and Samani 1985; Hargreaves and Allen 2003), which only uses maximum and minimum air temperature, in conjunction with local adjustment coefficients.

In Central Chile, irrigation scheduling is usually performed by estimating ET_{ref} using near-real-time meteorological information; i.e., using data from *today*, *yesterday* or the *previous week*. This method is well suited for low-frequency irrigation methods (furrow, basin, border irrigation, and impact sprinklers). However, for high-frequency irrigation methods (drip and micro-sprinkler irrigation) it is less efficient.

For high-frequency systems, which are associated with better control of water distribution and nutrient applications (fertigation) (Fares and Abbas 2009), and often lead to high yields and better crop quality (Madramootoo and Morrison 2013; Suryavanshi et al. 2015), scheduling irrigation for the upcoming days or week based on near-real-time ET_{ref} estimations can lead to deficits or excessive water use (Ben Hamouda et al. 2022). Thus, anticipating crop water requirements for the upcoming days through accurate ET_{ref} forecasts could lead to irrigation efficiency gains.

Thanks to important developments in computational technology and weather forecasting, in the last few decades ET_{ref} prediction has become an interesting topic for researchers (Luo et al. 2014, Perera et al. 2014, Yang et al. 2016, 2019a, 2019b, Liu et al. 2020, Granata and Di Nunno 2021, Ben Hamouda et al. 2022 and Zhang et al. 2022). Depending on the methodological approach and input data utilized, ET_{ref} predicting methods can be categorized as direct or indirect (Liu et al. 2020; Yang et al.

2016). Direct methods are based on the use of historical meteorological data and they are more appropriate for medium or long term ET_{ref} predictions (Yang et al. 2016). There are two main direct methods, namely the time series method and artificial neural networks. On the other hand, indirect methods use forecasts of weather variables in some ET models, such as the PM (Allen et al. 1998; Allen et al. 2005) or the HS model (Hargreaves and Samani 1985). These methods may be more useful for daily ET_{ref} forecasting (Yang et al. 2016).

Weather forecast models, typically accessible to the public, are especially valuable to the scientific community. A model that provides 384-hour (16 days) forecasts of nine meteorological variables (including those four involved in the PM equation) is the Global Forecast System 384-Hour Predicted Atmosphere Data, or simply, GFS (NOAA/NCEP 2022). The GFS is a coupled model produced by the National Centers for Environmental Prediction (NCEP) in the USA, composed of an atmosphere model, an ocean model, a land/soil model, and a sea ice model, which are operated jointly to forecast weather conditions. The forecasts generated by the GFS model can be processed using the Google Earth Engine (GEE) platform. The GFS is capable of producing spatially distributed data over the entire world, with a resolution of $27,830\ m$ pixels. This model has been the basis for research in different fields, including forecasting of wind speed (Zhao et al. 2016), precipitation (Yue et al. 2022), cloud properties (Yoo and Li 2012), bird migration (Van Doren and Horton 2018), intensity of hurricanes (Xue et al. 2013), transport and dispersion of pollutants in the atmosphere (Rolph et al. 2017), and also ET (Tian and Martinez 2012a, 2012b).

Considering that 80 % of Chile's irrigated agriculture takes place in the Mediterranean Central Zone of the country, the main goal of this work was to evaluate daily and cumulative ET_{ref} predictions for 1 to 7 days ahead, that are obtained from forecast weather variables generated by the GFS model (NOAA/NCEP 2022), for four different locations in the Central Valley of Chile. ET_{ref} was predicted using both the ASCE standardized PM (Allen et al.

2005) and HS (Hargreaves and Samani 1985) models over the course of three consecutive irrigation seasons (September-April of 2020-2022). The forecast ET_{ref} values were compared against ET_{ref} values calculated with the ASCE standardized PM equation using weather data collected at the four locations of the study, by automated weather stations.

3.2 Materials and methods

3.2.1 Study area and weather stations' locations

The Central Zone of Chile (Fig. 3.1) is one of the five natural regions into which the country is divided. Its limits are the Aconcagua River to the north and the Biobio River to the south, meanwhile to the east, it is bounded by the Andes Mountain Range, and to the west, by the Pacific Ocean. The Central Zone encompasses a plain composed by small valleys located between the Andes and Coastal Mountain Ranges. In this area, the climate is predominantly Warm-summer Mediterranean (Csb in the Köppen climate classification), with mild rainy winters, and dry and warm summers (Santibanez 2017).

Because the major part of irrigated agriculture in the country is concentrated in this zone, four weather stations located within different agroclimatic districts characterized by the Csb climate (Santibanez 2017), belonging to network Agrometeorologia (Chacon 2019), were selected for this study to evaluate the accuracy of ET_{ref} forecasts, namely Santa Rosa, San Clemente, El Tambo, and Los Tilos (Fig. 3.1).

Figure 3.1: Central Zone of Chile (limited by the Aconcagua River to the north, the Biobio River to the south, the Andes Mountain Range to the east and the Pacific Ocean to the west) with the location of the four weather stations selected for the present study (red dots; with latitude, longitude and elevation, respectively), in four administrative regions (Reg., black lines), with its capital Santiago (black square).

The monthly averages of daily maximum and minimum air temperature, incoming solar radiation, mean relative humidity, and mean wind speed for these four locations during the irrigation seasons (September to April) of the three-year period 2020-2022 in this study are shown in Figs. 3.10 to 3.13, of Appendix A.

3.2.2 The ASCE standardized reference evapotranspiration equation

The most widely accepted method for reference ET calculation is the PM model (Allen et al. 1998; Allen et al. 2005; Reichardt and Timm 2020). The model has a solid physical basis and includes physiological aspects of the plants. Meteorological variables considered are incoming solar radiation, air temperature, atmospheric humidity and wind speed. It also incorporates the albedo and the surface and aerodynamic resistances of the crop.

The ASCE Standardized Reference Evapotranspiration Equation (Allen et al. 2005), a method for calculating $ET_{ref} = ET_{sz}$ (daily or hourly), standardizes the use of the PM equation. The ASCE ET_{sz} computation procedure has been defined for two reference crops: a short one, with an approximate height of 12 cm (like a clipped cold season pasture grass); and a tall one, with an approximate height of 50 cm (like a full cover alfalfa). For the short crop, ET_{sz} is denoted as ET_{os}, while for the tall crop as ET_{rs}.

The daily $ET_{os}(mm\, d^{-1})$ is determined by the standardized PM equation (Allen et al. 2005):

$$ET_{os} = \frac{0.408\Delta\,(R_n - G) + \gamma \frac{C_n}{T+273} u_2\,(e_s - e_a)}{\Delta + \gamma\,(1 + C_d u_2)} \tag{3.1}$$

where $R_n\ (MJ\ m^{-2}\ d^{-1})$ is the net radiation; $G\ (MJ\ m^{-2}\ d^{-1})$ is the ground heat flux; $T\ (^{\circ}C)$ is the mean daily air temperature at 1.5 to 2.5 m height; $u_2\ (m\ s^{-1})$ is the mean daily wind speed at 2 m height; $e_s\ (kPa)$ is the saturation vapor pressure at 1.5 to 2.5 m height, calculated as the average of saturation vapor pressure at maximum and minimum daily air temperature; $e_a\ (kPa)$ is the mean actual vapor pressure at 1.5 to 2.5 m height; $\Delta(kPa^{\circ}C^{-1})$ is the slope of the saturation vapor pressure-temperature curve; $\gamma\,(kPa^{\circ}C^{-1})$ is the psychrometric constant; $C_n = 900$ is a dimensionless constant depending on

aerodynamic roughness of the surface; $C_d = 0.34$ is a dimensionless constant depending on bulk surface resistance and aerodynamic roughness of the surface; and 0.408 is a coefficient with units $m^2\ mm\ MJ^{-1}$.

For each of the terms in Eq. (3.1), the ASCE proposes one or more calculations procedures, whose application will depends on the reliability or availability of meteorological data (Allen et al., 2005).

Thus, daily air temperature is estimated as the mean of the daily maximum and daily minimum air temperatures, T_{max} and T_{min}, as:

$$T = \frac{T_{max} + T_{min}}{2} \tag{3.2}$$

The psychrometric constant is proportional to the mean atmospheric pressure $P\,(kPa)$ at station elevation $z\,(m)$, and it is calculated as:

$$\gamma = 0.000665P \tag{3.3}$$

where:

$$P = 101.3\left(\frac{293 - 0.0065z}{293}\right)^{5.26} \tag{3.4}$$

The slope of the saturation vapor pressure-temperature curve is computed as:

$$\Delta = \frac{2503}{(T + 237.3)^2}\exp\left(\frac{17.27\,T}{T + 237.3}\right) \tag{3.5}$$

In the ASCE standardized procedure, the saturation vapor pressure is given by:

$$e_s = \frac{e^o(T_{max}) + e^o(T_{min})}{2} \tag{3.6}$$

where:

$$e^o(T_{max}) = 0.6108\exp\left(\frac{17.27\,T_{max}}{T_{max} + 237.3}\right) \tag{3.7}$$

and

$$e^o(T_{min}) = 0.6108 \exp\left(\frac{17.27\, T_{min}}{T_{min} + 237.3}\right) \tag{3.8}$$

To compute e_a in the daily ET_{os} PM equation, the ASCE proposes several methods, of which the most preferred is the one using hourly relative humidity $RH_h\ (\%)$ and hourly air temperature $T_h\ (^\circ C)$ data. Thus, e_a is obtained as the average over the daily period of the hourly actual vapor pressure (e_{ah}):

$$e_{ah} = \frac{RH_h\, e^o(T_h)}{100} \tag{3.9}$$

where $e^o(T_h)$ is saturation vapor pressure function:

$$e^o(T_h) = 0.6108 \exp\left(\frac{17.27\, T_h}{T_h + 237.3}\right) \tag{3.10}$$

The calculation of net radiation includes two components, net short-wave radiation $R_{ns}\ (MJ\, m^{-2}\, d^{-1})$ and net long-wave radiation $R_{nl}\ (MJ\, m^{-2}\, d^{-1})$:

$$R_n = R_{ns} - R_{nl} \tag{3.11}$$

Net short-wave radiation results from the balance between incoming and reflected solar radiation, and is given by:

$$R_{ns} = R_s - \alpha\, R_s = (1 - \alpha)\, R_s \tag{3.12}$$

where $R_s (MJ\, m^{-2}\, d^{-1})$ is the incoming solar radiation and $\alpha (dimensionless)$ is the albedo of the canopy, which is set at 0.23 for the standardized short and tall reference surfaces.

Net long-wave radiation is the difference between upward long-wave radiation from the standardized surface and downward long-wave radiation from the sky, and it is calculated

using the equation:

$$R_{nl} = \sigma \, f_{cd} \, (0.34 - 0.14 \sqrt{e_a}) \, \frac{(T_{Kmax}^4 + T_{Kmin}^4)}{2} \tag{3.13}$$

where $\sigma = 4.901 \times 10^{-9} \, MJ \, K^{-4} \, m^{-2} \, d^{-1}$ is the Stefan-Boltzmann constant, $T_{Kmax} \, (K)$ and $T_{Kmin} \, (K)$ are the maximum and minimum temperatures in the Kelvin scale, and $f_{cd} \, (dimensionless)$ is the cloudiness function (limited to $0.05 \leq f_{cd} \leq 1.0$):

$$f_{cd} = 1.35 \, \frac{R_s}{R_{so}} - 0.35 \tag{3.14}$$

where $R_{so} \, (MJ \, m^{-2} \, d^{-1})$ represents the clear-sky radiation, which is computed based on the Earth's position relative to the sun and the specific location's latitude (Allen et al. 2005).

Since it is not always possible to have the wind speed at $2 \, m$ from the ground, the ASCE suggests the use of the following logarithmic equation to adjust the wind speed $u_z \, (m \, s^{-1})$ measured at the height $z_w \, (m)$:

$$u_2 = u_z \, \frac{4.87}{\ln 67.8 \, z_w - 5.42} \tag{3.15}$$

Note that this equation is only an approximation and, in certain cases, a more general equation must be considered (see Eq. (3.19)).

Regarding the daily soil heat flux density, it is common to consider the approximation:

$$G = 0 \tag{3.16}$$

as its magnitude is negligible compared to R_n.

Thus, for a given location (for example, those of the selected weather stations), observed and predicted daily ET_{os} can be obtained by using measured and predicted meteorological data in Eqs. (3.1) to (3.16), respectively.

3.2.3 The Hargreaves-Samani reference evapotranspiration equation

Since it is not always feasible to obtain a complete and reliable dataset for the four meteorological variables that are utilized to calculate ET_{ref} with the PM method, it is sometimes convenient to use alternative models. One such model is the HS Model (Hargreaves and Samani 1985; Hargreaves and Allen 2003), which offers a simplified approach to estimate ET_{ref} using only minimum and maximum air temperatures. This model has shown reasonable accuracy and applicability under various climatic conditions (Hargreaves and Allen 2003), being utilized with adjustment coefficients.

In this framework, the incident solar radiation is calculated with the equation:

$$R_s = k_{RS}\sqrt{T_{max} - T_{min}}\, R_a \tag{3.17}$$

where $R_a\ (MJ\, m^{-2}\, d^{-1})$ is the extraterrestrial radiation, defined as the short-wave solar radiation in the absence of an atmosphere, which is a function of the day of the year, time of day, and latitude; and $k_{RS}\ (^{\circ}C^{-0.5})$ is the radiation adjustment coefficient, which is empirically determined and differs for interior ($\approx 0.16\ ^{\circ}C^{-0.5}$) and coastal regions ($\approx 0.19\ ^{\circ}C^{-0.5}$) (Allen et al. 1998).

To obtain the daily $ET_{ref} = ET_{oHS}$ equation in the HS model, the incident solar radiation Eq. (3.17) is multiplied by an empirical local adjustment coefficient $k_L\ (^{\circ}C^{-1})$ and a linear function on the mean daily temperature T:

$$ET_{oHS} = \frac{k_L\, k_{RS}}{\lambda}\sqrt{T_{max} - T_{min}}\, R_a\, (T + 17.8) \tag{3.18}$$

where $\lambda = 2.45\ MJ\ kg^{-1}$ is the latent heat of water vaporization, introduced to express ET_{oHS} in units of $mm\ day^{-1}$. Typically, k_L is 0.0135 (Hargreaves and Samani 1985).

Thus, with the HS model, ET_{ref} forecast can be obtained using only temperature predictions, which represents a remarkable simplification with respect to the PM model.

3.2.4 Data collection

Meteorological data were collected at the four weather stations through the Agrometeorologia online system (Chacon, 2019). This network consists of a number of automated agrometeorological station distributed throughout Chile and includes a system for capturing and recording agrometeorological data remotely, which are available to the public on the web site https://agrometeorologia.cl. In order to calculate ET_{os} from measurements of weather variables and using Eq. (3.1), for each of the four stations in Fig. 3.1, hourly data were obtained for incident solar radiation, air temperature, relative humidity, and wind speed, for the irrigation seasons over a 3-year period, spanning from 2020 to 2022.

For the same period, and selecting the pixels that contain the four weather stations' locations, the meteorological forecasts provided by the GFS in GEE were extracted. The pixel size is $27,830\ m \times 27,830\ m$; and the 384-hour forecasts, with 1-hour (up to 120 hours) and 3-hour (after 120 hours) forecast intervals, are given at a 6-hour temporal resolution, updated four times per day. In this paper, only one (the first one) of these four daily updates was considered. Since forecasts for times above 120 hours have 3-hours inverval, it was necessary to impute the missing values, in order to complete the hourly dataset. The imputation of data was performed with the RStudio package imputeTS: Time Series Missing Value Imputation (Moritz and Bartz-Beielstein 2017), using a cubic spline interpolation method. Thus, the 7-days ET_{ref} forecasts were obtained by evaluating the GFS predicted and imputed data in Eqs. (3.1) and (3.18).

Note that wind speed predictions provided by the GFS model refer to a height of $10\ m$ above the ground. To satisfy the requirement of the ASCE standardized ET_{ref} equation, was necessary to derive the wind speed values at $2\ m$ above the ground. For this purpose, the full logarithmic wind speed profile equation (B.14) was used as reported in the Appendix

B of Allen et al. (2005):

$$u_2 = u_z \frac{ln\left(\frac{2-d}{z_{om}}\right)}{ln\left(\frac{z_w-d}{z_{om}}\right)} \tag{3.19}$$

where $u_2\ (m\ s^{-1})$ is the wind speed at $2\ m$ above ground surface; $u_z\ (m\ s^{-1})$ is the wind speed at height $z_w\ (m)$ above ground surface; $d\ (m)$ is the zero plane displacement height for the vegetation ($d = 0.67\ h$); $z_{om}\ (m)$ is the aerodynamic roughness length for the vegetation ($z_{om} = 0.123\ h$); and $h\ (m)$ is the vegetation height. Due to the pixel size in the GFS model, this height needs to be adjusted to obtain adequate ET_{ref} forecasts. After examining the area surrounding the four stations, a vegetation height of $h = 1.7\ m$ was settled for the entire pixel.

3.2.5 Evaluation of ET_{ref} forecasts

In this paper single-day, and cumulative ET_{ref} forecast for prediction times ranging from 1 to 7 days were assessed. While single-day ET_{ref} forecasts were obtained directly from Eqs. (3.1) and (3.18), cumulative ET_{ref} forecasts up to a specific day were calculated by simply adding several single-day forecasts from previous days.

In addition to the graphical evaluation of single-day and cumulative ET_{ref} forecasts with time series and 1:1 plots, statistical indices were used to assess the performance of the models. The evaluation of forecast ET_{ref} values is mainly based on the root mean square error ($RMSE$), the normalized root mean square error ($NRMSE$), the mean bias error (MBE) and the normalized mean bias error ($NMBE$). These indices are defined by the Eqs. (3.20) through (3.23) presented hereafter (Wilks 2005):

$$RMSE = \sqrt{\frac{1}{n}\sum_{i=1}^{n}(x_i - y_i)^2} \tag{3.20}$$

$$NRMSE = \frac{RMSE}{\bar{y}}\ 100\% \tag{3.21}$$

$$MBE = \frac{1}{n}\sum_{i=1}^{n}(x_i - y_i) \tag{3.22}$$

$$NMBE = \frac{MBE}{\bar{y}}\,100\% \tag{3.23}$$

where x_i is a forecast value; y_i is an observed value; i is the forecast/observed sample sequence number $i = 1, 2, ..., n$; n is the number of forecast/observed data; $\bar{x}$ is the average of forecast values of the sample; and $\bar{y}$ is the average of observed values of the sample.

Another indicator used to evaluate only daily ET_{ref} forecasts is the $Accuracy$ (Luo et al. 2014; Zhang et al. 2022), which is defined in the present article as the percentage of ET_{ref} predictions having an absolute error less than or equal to $1\ mm\ d^{-1}$. Of course, it is desirable that the $Accuracy$ be as close as possible to $100\,\%$. Note that in Luo et al. (2014) and Zhang et al. (2022) $Accuracy$ was defined considering an absolute error value of $1.5\ mm\ d^{-1}$, instead of $1\ mm\ d^{-1}$. In addition, the coefficient of determination (R^2) was also calculated.

3.2.6 Evaluation of air temperature, incoming solar radiation, relative humidity and wind speed forecasts from GFS

Not only evaluating ET_{ref} forecasts is important, but also assessing the performance of GFS forecasts for the four fundamental meteorological variables: incoming solar radiation, air temperature, relative humidity, and wind speed. To achieve this, the statistical indicators defined in Eqs. (3.20)-(3.23) were used for the four weather stations' location considered in this study.

The results, summarized for each weather station in Tables 3.5 to 3.8 in Appendix A, show a satisfactory performance for the temperature forecasts, with 7-day averages of the $NRMSE$ ranging between 12.1 % and 16.8 % in the mean daily temperature. Daily incoming solar radiation was overestimated, as indicated by the 7-day averages of $NMBE$,

ranging between 23.5 % and 35.1 %. Relative humidity forecasts were underestimated, with the 7-day averages of $NMBE$ in the range between -15.2 % and -23.3 %. On the other hand, wind speed forecasts were overestimated, with the set of statistical indicators not showing a good fit, which may be due to the large size of the GFS pixel and the conditions at the weather stations' locations.

Thus, the overestimation of incoming solar radiation and wind speed forecasts, as well as the underestimation of relative humidity predictions, allows us to anticipate an overestimation of ET_{ref} forecasts, using the PM equation. However, the HS model, which is only dependent on temperature, could provide more accurate ET_{ref} predictions.

3.2.7 Notation

In this work ET_{ref} represents reference ET in the most general way, including here its utilization for PM and HS or any other estimation models, evaluated using either measured or forecasted weather data, for the two types of surfaces: short or tall canopy.

The term ET_{os} will denote the reference ET of the short canopy calculated using the ASCE standardized PM equation. Specifically, when ET_{os} is obtained from measured weather data, the superindex m (measured, or observed) will be included: ET_{os}^{m}. Whereas, when ET_{os} is obtained from forecasted weather data, the superindex f (forecasted, or predicted) will be used: ET_{os}^{f}.

ET_{oHS} will be used for the reference ET of a short crop estimated using the HS model. Then, when we want to emphasize that ET_{oHS} was obtained from forecasted meteorological variables, we will add the superindex f: ET_{oHS}^{f}.

In addition, while there will be no special notation to distinguish between daily and cumulative ET_{ref} (ET_{os} or ET_{oHS}), it will always be explicitly stated whether it is one or the other.

3.3 Results and discussion

3.3.1 Evaluation of ET_{os} forecasts based on air temperature, relative humidity, wind speed and solar radiation predictions from GFS

Single-day and cumulative ET_{os} forecasts from GFS meteorological data predictions were computed and compared against values obtained from weather variables measured at the four selected stations.

Fig. 3.2 illustrates single-day ET_{os}^{f} forecasts obtained using the ASCE's preferred method of computation for the four weather stations over the course of the irrigation season for the period of 2020 through 2022. Although time series for all forecast days in the range 1 to 7 were made, only two of them are displayed in Fig. 3.2 to enhance graphical representation. These plots contrast the predicted daily ET_{os}^{f} with the observed daily ET_{os}^{m}, revealing an overestimation of predicted values. This overestimation is also depicted in the 1:1 plots of Fig. 3.3. The El Tambo station is an exceptional one, given that the overestimation of ET_{os}^{f} forecasts is not as evident as for the other three stations' locations.

On the other hand, time series for one week cumulative ET_{os}^{f} forecast along the irrigation season for the period of 2020 through 2022 are shown in Fig. 3.4. The corresponding 1:1 plots, which compare ET_{os}^{f} forecasts obtained from predictions of meteorological variables with ET_{os}^{m} obtained from measurements of meteorological variables, are displayed in Fig. 3.5. As occurs for the single-day forecasts, the cumulative ET_{os}^{f} forecast also exhibits some overestimation.

Table 3.1 presents values of the statistical indices calculated for the single-day ET_{os}^{f} forecasts conducted for the four weather stations covering the period from 1 to 7 days. For the same time span, the statistical indicators for the cumulative ET_{os}^{f} predictions are shown in Table 3.2.

Across all the weather stations, the values of statistical indicators for Santa Rosa, San Clemente, and Los Tilos reveal inadequate forecast performance. For these stations, the

7-day average of the $Accuracy$ ranges between 35.4 % and 42.8 %; i.e., approximately 60 % of the times, ET_{os}^{f} forecasts deviate by more than 1 $mm\,d^{-1}$ from ET_{os}^{m} measured. Thus, scheduling irrigation based on these numbers seems inappropriate, requiring to explore alternative approaches that could yield better performance (see Subsec. 3.3.2).

The 7-day average $RMSE$ for single-day ET_{os}^{f} for the three stations falls within the range 1.36 $mm\,d^{-1}$ to 1.68 $mm\,d^{-1}$, significantly exceeding the 1 $mm\,d^{-1}$ threshold considered for the $Accuracy$. Additionally, the MBE indicates an overestimation in daily ET_{os}^{f} also exceeding 1 $mm\,d^{-1}$, with a $NMBE$ ranging from 28.0 % to 36.9 %. At the same time, the 7-day average of the coefficient of determination R^2 ranges from 0.75 to 0.79.

For these three stations, the indicators of cumulative ET_{os}^{f} forecasts exhibit similar behavior. For 7-day cumulative forecasts, an overestimation in the range 27.9 % to 36.9 % was observed in the $NMBE$, while the $RMSE$ ranges between 8.71 mm and 10.99 mm, representing a value of the $NRMSE$ of 31.6 % to 42.0 %. Additionally, the coefficient of determination is around 0.90.

In addition, El Tambo station shows notably more favorable performance. For single-day ET_{os}^{f} predictions, the 7-day average of $Accuracy$, $RMSE$, $NRMSE$, MBE, $NMBE$, and R^2 are 77.8 %, 0.95 $mm\,d^{-1}$, 21.5 %, 0.40 $mm\,d^{-1}$, 9.1 %, and 0.72, respectively. For this station, the one-week cumulative ET_{os}^{f} forecast indices yield a $RMSE$ of 4.80 mm, $NRMSE$ of 15.4 %, MBE of 2.84 mm, $NMBE$ of 9.1 %, and R^2 of 0.87.

The comprehensive analysis of these results suggests that the ET_{os}^{f} forecasts, derived from GFS meteorological predictions and the ASCE model, exhibit performance levels that are aligned with the statistical indicators associated with weather variable forecasts (Tables 3.5 to 3.8). In particular, the indicators MBE and $NMBE$ in Tables 3.1 and 3.2 reveal an overestimation in ET_{os}^{f} predictions for the four stations. This may be explained by considering that an overestimation of wind speed and incoming solar radiation (and consequently, on net radiation), and an underestimation of relative humidity (and

consequently, on actual vapor pressure), lead these three conditions to an increase in ET_{os}^{f}.

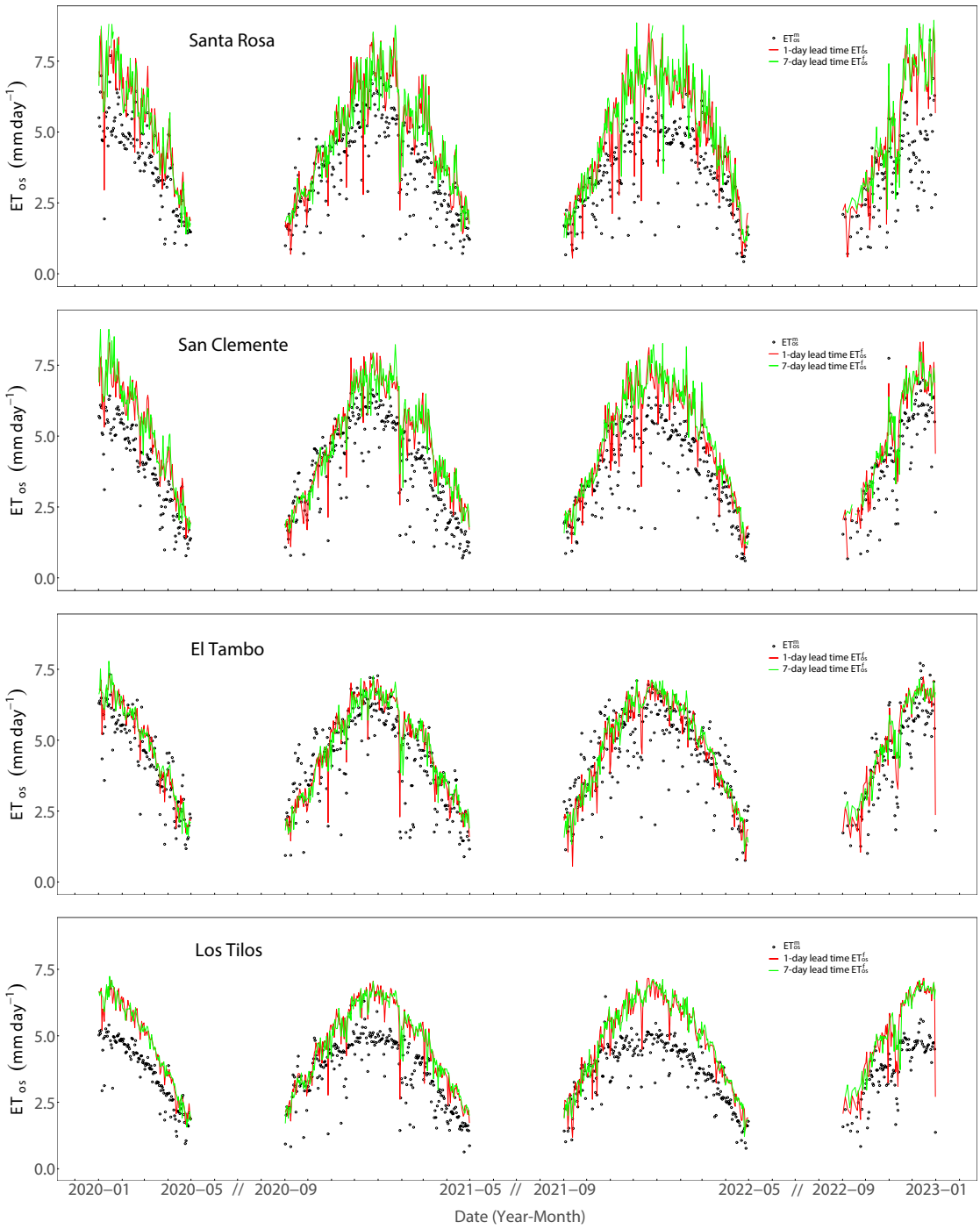

Figure 3.2: Forecasted daily standardized reference evapotranspiration using the ASCE method from Global Forecast System 1 and 7-day ahead meteorological data predictions (ET_{os}^{f}) and from measured weather variables (ET_{os}^{m}), for Santa Rosa, San Clemente, El Tambo and Los Tilos weather stations over the course of the irrigation season (September to April) for the period of 2020 through 2022.

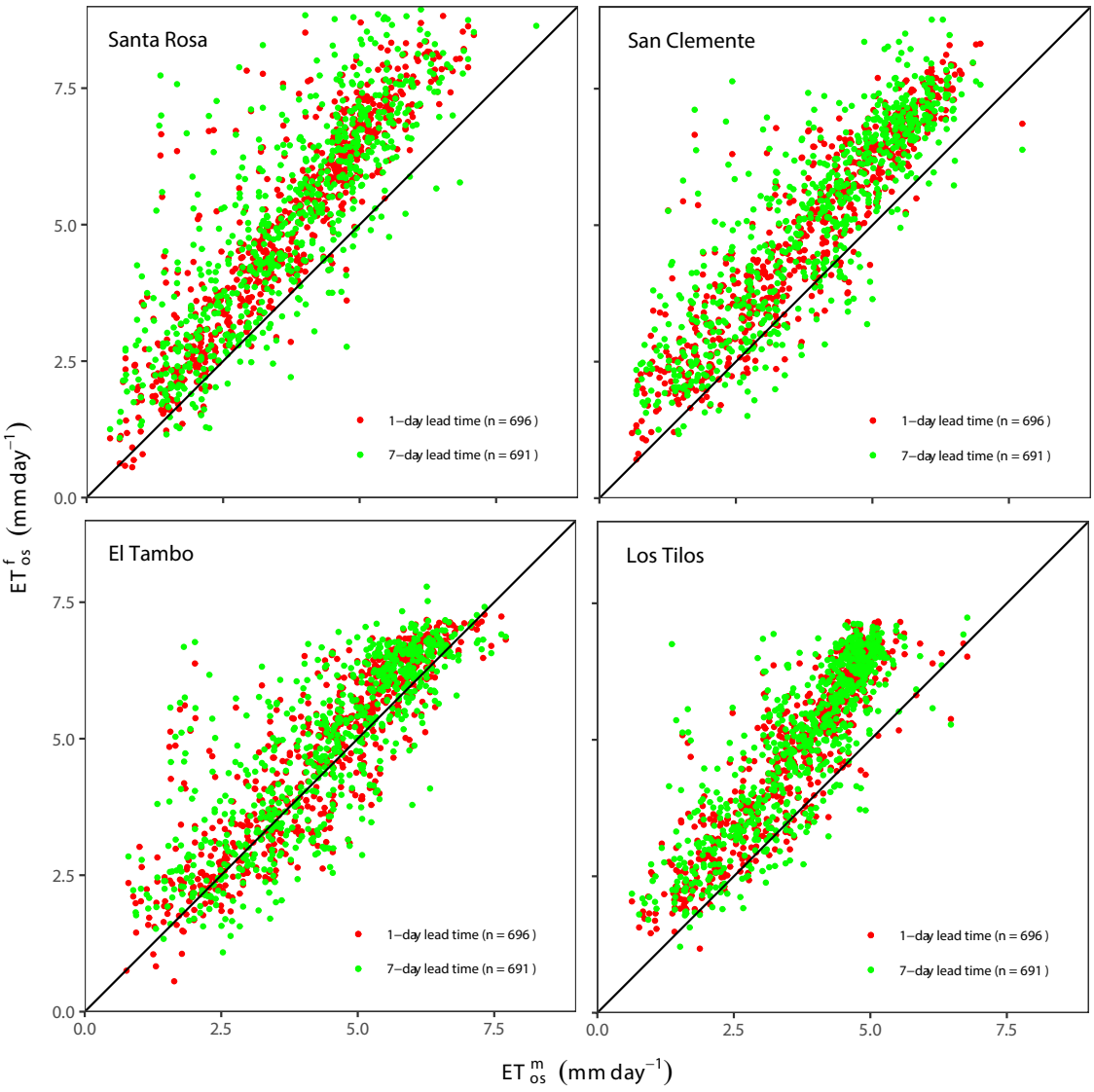

Figure 3.3: 1:1 ratio of forecasted daily standardized reference evapotranspiration using the ASCE method from Global Forecast System 1 and 7-day ahead meteorological data predictions (ET_{os}^{f}) and from measured weather variables (ET_{os}^{m}), for Santa Rosa, San Clemente, El Tambo, and Los Tilos weather stations along the irrigation season (September through April) for the period of 2020 through 2022.

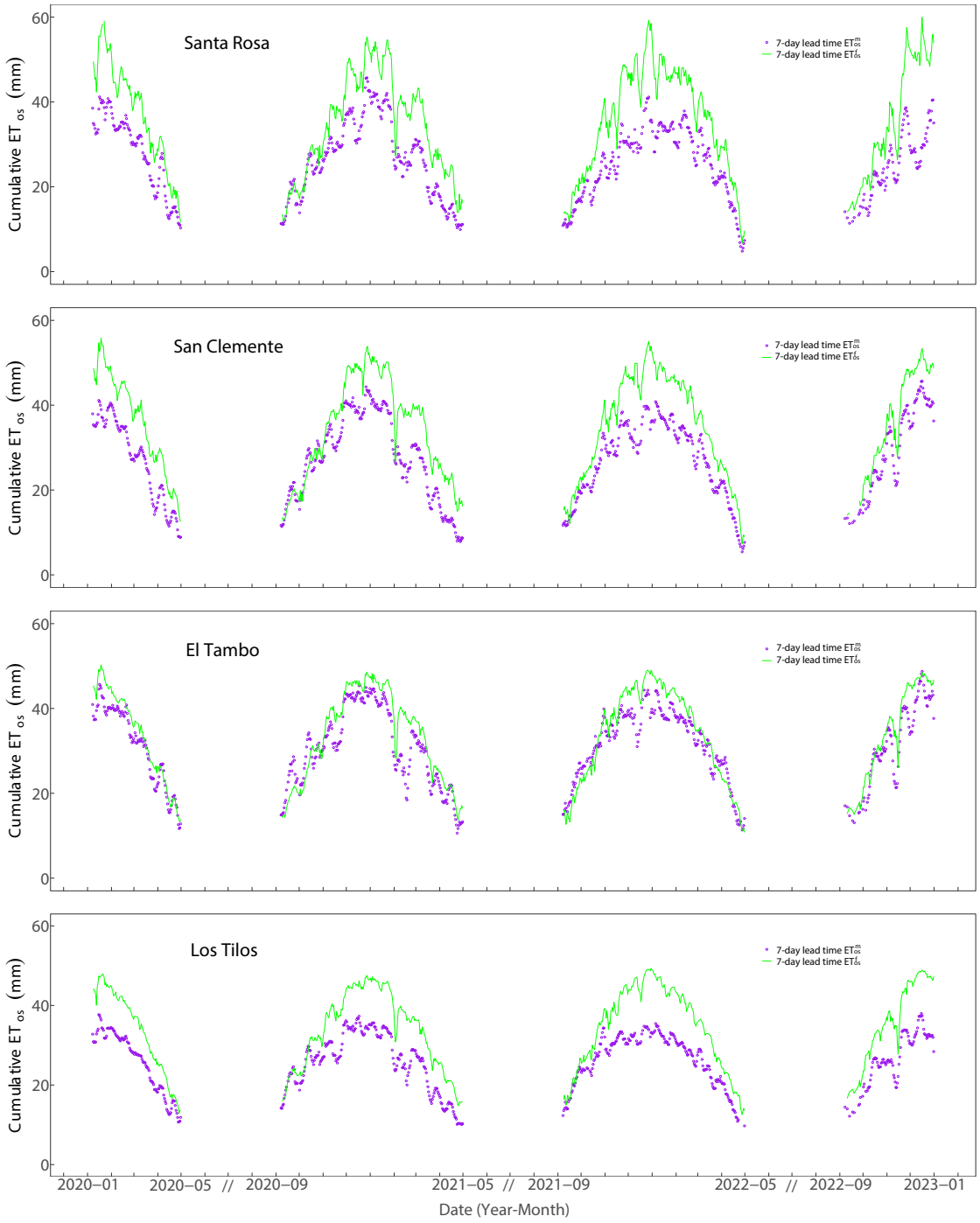

Figure 3.4: Forecasted cumulative 7-day standardized reference evapotranspiration using the ASCE method from Global Forecast System 7-day ahead meteorological data predictions (ET_{os}^{f}) and from measured weather variables (ET_{os}^{m}), for Santa Rosa, San Clemente, El Tambo and Los Tilos weather stations along the irrigation season (September through April) for the period of 2020 through 2022.

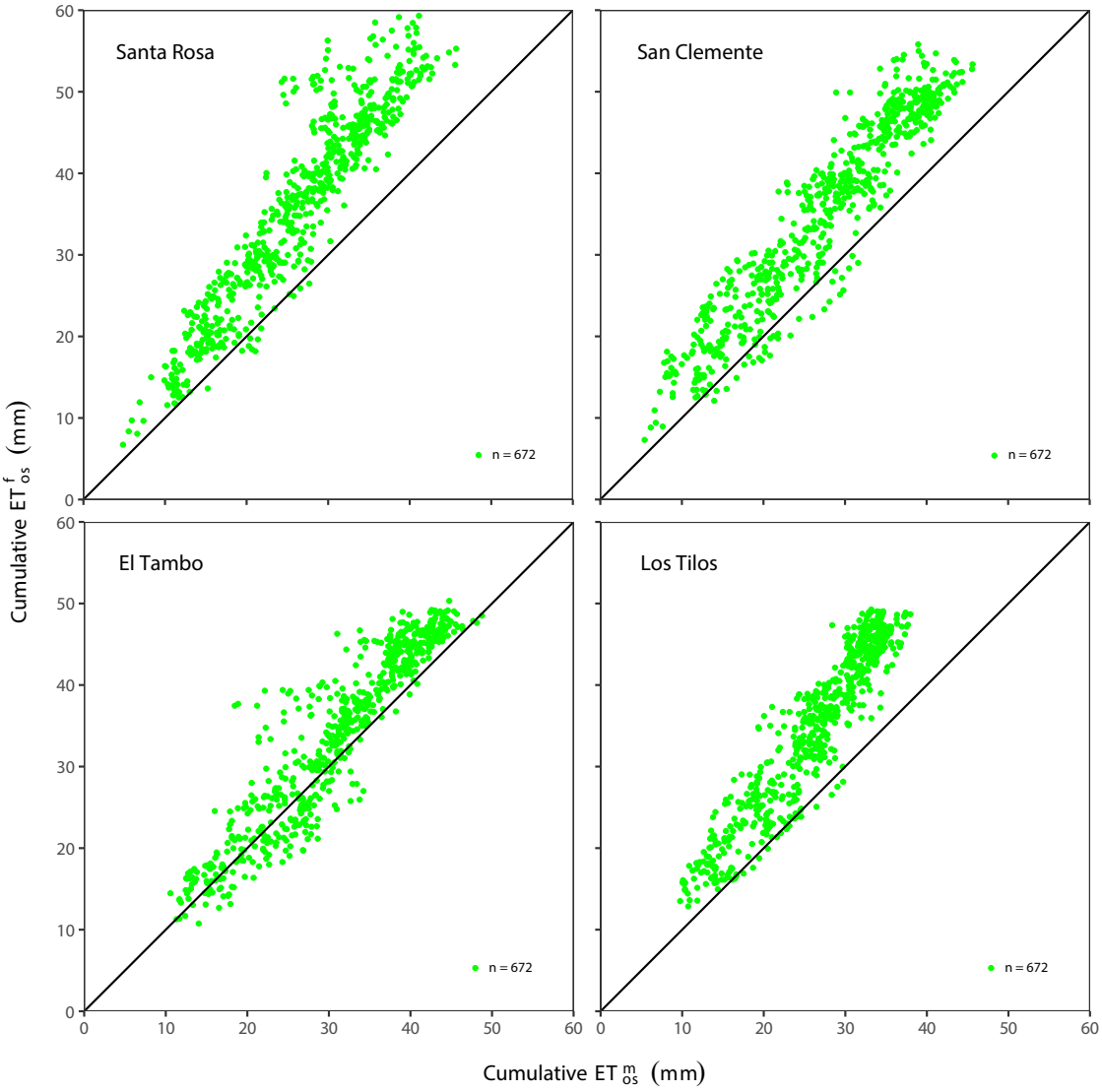

Figure 3.5: 1:1 ratio of forecasted cumulative 7-day standardized reference evapotranspiration using the ASCE method from Global Forecast System 7-day ahead meteorological data predictions (ET_{os}^{f}) and from measured weather variables (ET_{os}^{m}), for Santa Rosa, San Clemente, El Tambo, and Los Tilos weather stations along the irrigation season (September through April) for the period of 2020 through 2022.

Table 3.1: Statistical indices of forecasted daily standardized reference evapotranspiration using the ASCE method from Global Forecast System 1 to 7-day ahead meteorological data predictions (ET_{os}^{f}) compared with values obtained from measured weather variables (ET_{os}^{m}), for Santa Rosa, San Clemente, El Tambo and Los Tilos weather stations along the irrigation season (September through April) for the period of 2020 through 2022.

Santa Rosa						
Day of forecast	$Accuracy$ (%)	$RMSE$ (mm d^{-1})	$NRMSE$ (%)	MBE (mm d^{-1})	$NMBE$ (%)	R^2
1	36.9	1.56	42.4	1.31	35.5	0.82
2	35.4	1.61	43.5	1.34	36.1	0.79
3	35.7	1.63	43.7	1.34	36.1	0.79
4	35.5	1.66	44.8	1.36	36.8	0.77
5	34.2	1.72	46.4	1.40	37.8	0.74
6	35.1	1.77	47.7	1.41	38.1	0.69
7	35.0	1.81	48.7	1.41	38.0	0.66
Average	35.4	1.68	45.3	1.37	36.9	0.75

San Clemente						
Day of forecast	$Accuracy$ (%)	$RMSE$ (mm d^{-1})	$NRMSE$ (%)	MBE (mm d^{-1})	$NMBE$ (%)	R^2
1	43.3	1.26	32.5	1.04	26.9	0.85
2	42.7	1.30	33.5	1.06	27.4	0.82
3	41.9	1.32	33.7	1.07	27.5	0.82
4	44.7	1.35	34.8	1.09	28.0	0.79
5	43.7	1.39	35.7	1.09	28.2	0.78
6	42.2	1.45	37.4	1.14	29.3	0.74
7	41.0	1.47	37.7	1.14	29.2	0.73
Average	42.8	1.36	35.1	1.09	28.0	0.79

El Tambo						
Day of forecast	$Accuracy$ (%)	$RMSE$ (mm d^{-1})	$NRMSE$ (%)	MBE (mm d^{-1})	$NMBE$ (%)	R^2
1	81.5	0.86	19.6	0.37	8.4	0.77
2	79.6	0.90	20.5	0.39	8.8	0.75
3	79.8	0.88	20.0	0.38	8.6	0.76
4	78.2	0.93	21.2	0.40	9.1	0.73
5	76.5	0.98	22.2	0.40	9.2	0.71
6	74.7	1.04	23.6	0.45	10.1	0.67
7	74.1	1.05	23.7	0.41	9.3	0.65
Average	77.8	0.95	21.5	0.40	9.1	0.72

Los Tilos						
Day of forecast	$Accuracy$ (%)	$RMSE$ (mm d^{-1})	$NRMSE$ (%)	MBE (mm d^{-1})	$NMBE$ (%)	R^2
1	38.3	1.34	36.7	1.16	31.7	0.82
2	38.3	1.38	37.5	1.18	32.2	0.80
3	36.5	1.39	37.8	1.20	32.6	0.80
4	34.6	1.42	38.7	1.21	33.1	0.77
5	35.4	1.42	38.8	1.21	32.9	0.77
6	35.8	1.46	39.8	1.22	33.2	0.71
7	35.9	1.46	39.6	1.21	32.8	0.70
Average	36.4	1.41	38.4	1.20	32.6	0.77

$RMSE$: Root mean square error; $NRMSE$: Normalized root mean square error; MBE : Mean bias error; $NMBE$: Normalized mean bias error; R^2 : Coefficient of determination.

Table 3.2: Statistical indices of forecasted cumulative 1 to 7-day standardized reference evapotranspiration using the ASCE method from Global Forecast System 1 to 7-day ahead meteorological data predictions (ET_{os}^{f}) compared with values obtained from measured weather variables (ET_{os}^{m}), for Santa Rosa, San Clemente, El Tambo and Los Tilos weather stations along the irrigation season (September through April) for the period of 2020 through 2022.

Santa Rosa					
Day of forecast	$RMSE$ (mm)	$NRMSE$ (%)	MBE (mm)	$NMBE$ (%)	R^2
1	1.56	42.4	1.31	35.5	0.82
2	3.09	41.8	2.65	35.8	0.84
3	4.63	41.5	4.00	35.9	0.86
4	6.18	41.5	5.38	36.1	0.87
5	7.75	41.6	6.79	36.5	0.87
6	9.36	41.8	8.23	36.7	0.87
7	10.99	42.0	9.66	36.9	0.87

San Clemente					
Day of forecast	$RMSE$ (mm)	$NRMSE$ (%)	MBE (mm)	$NMBE$ (%)	R^2
1	1.26	32.5	1.04	26.9	0.85
2	2.47	31.8	2.11	27.1	0.87
3	3.69	31.5	3.19	27.2	0.88
4	4.91	31.4	4.29	27.4	0.89
5	6.14	31.3	5.40	27.5	0.90
6	7.42	31.5	6.54	27.8	0.90
7	8.71	31.6	7.69	27.9	0.90

El Tambo					
Day of forecast	$RMSE$ (mm)	$NRMSE$ (%)	MBE (mm)	$NMBE$ (%)	R^2
1	0.86	19.6	0.37	8.4	0.77
2	1.58	18.0	0.76	8.6	0.81
3	2.21	16.7	1.14	8.6	0.83
4	2.84	16.0	1.55	8.8	0.85
5	3.48	15.7	1.96	8.9	0.86
6	4.15	15.6	2.42	9.1	0.87
7	4.80	15.4	2.84	9.1	0.87

Los Tilos					
Day of forecast	$RMSE$ (mm)	$NRMSE$ (%)	MBE (mm)	$NMBE$ (%)	R^2
1	1.34	36.7	1.16	31.7	0.82
2	2.67	36.3	2.35	31.9	0.85
3	4.01	36.1	3.57	32.2	0.87
4	5.35	36.2	4.79	32.4	0.88
5	6.69	36.1	6.02	32.4	0.88
6	8.06	36.1	7.27	32.5	0.89
7	9.42	36.0	8.50	32.5	0.89

$RMSE$: Root mean square error; $NRMSE$: Normalized root mean square error; MBE : Mean bias error; $NMBE$: Normalized mean bias error; R^2 : Coefficient of determination.

3.3.2 Evaluation of ET_{oHS} forecasts based on air temperature predictions from GFS

For the four weather stations, air temperature forecasts show superior performance compared to those of incident solar radiation, wind speed, and relative humidity variables (Tables 3.5 to 3.8). Then, predicting ET_{ref} with the HS equation (3.18), which utilizes only temperature as input variable, seems a good option. Since the selected weather stations are located inland of Central Chile (Fig. 3.1), the solar radiation adjustment coefficient $k_{RS} = 0.16\,°C^{-0.5}$ in the HS equation was chosen (Allen et al. 1998). Furthermore, the local adjustment coefficient k_L was picked to maximize the $Accuracy$ indicator in ET^f_{oHS} forecasts, considering numbers with three decimal places; thus, $0.010\,°C^{-1}$ was selected for Santa Rosa, San Clemente and Los Tilos weather stations, and $0.011\,°C^{-1}$ was chosen for El Tambo weather station.

Using the HS model, significant improvements on the ET_{ref} forecasts were achieved. In the time series presented in Fig. 3.6, 1-day and 7-day ET^f_{oHS} forecasts obtained using the HS approach, for the four weather stations and along the irrigation seasons in the period 2020-2022, are shown (also, the observed ET^m_{os} obtained using the ASCE standardized PM equation). These forecasts, compared to those presented in Fig. 3.2, exhibit a considerably improved fit. This is also reflected in the 1:1 plots associated with these forecasts (Fig. 3.7), which no longer show noticeable overestimation. Similarly, the corresponding time series to the 7-day cumulative ET^f_{oHS} (Fig. 3.8) and the 1:1 plots (Fig. 3.9) also show a good fit.

The statistical indicators presented in the Tables 3.3 and 3.4 reveal enhanced forecasts for ET^f_{oHS} over the 1-day to 7-day led times.

Thus, for the single-day ET^f_{oHS} forecast at the Santa Rosa weather station, the 7-day average of $Accuracy$, $RMSE$, $NRMSE$, MBE, $NMBE$ and R^2 indicators are 78.6 %, 0.89 $mm\,d^{-1}$, 24.1 %, 0.11 $mm\,d^{-1}$, 3.0 % and 0.66, respectively. For the 7-day cumulative

ET^f_{oHS} forecast in the same station, the values $RMSE$, $NRMSE$, MBE, $NMBE$ and R^2 yield 3.60 mm, 13.8 %, 0.77 mm, 3.0 % and 0.85, respectively. These results represent a clear improvement in $Accuracy$, $RMSE$, $NRMSE$, MBE and $NMBE$ compared to the previous case (Tables 3.1 and 3.2). On the other hand, the coefficient of determination R^2 shows a weaker performance.

Similar results were obtained at the San Clemente station. The 7-day average in the single-day ET^f_{oHS} forecasts for the $Accuracy$, $RMSE$, $NRMSE$, MBE, $NMBE$ and R^2 are 80.4 %, 0.83 $mm\,d^{-1}$, 21.3 %, 0.10 $mm\,d^{-1}$, 2.5 % and 0.73, respectively. For the one-week cumulative ET^f_{oHS} forecast the values $RMSE$, $NRMSE$, MBE, $NMBE$ and R^2 are 3.86 mm, 14.0 %, 0.66 mm, 2.4 % and 0.85, respectively.

The best forecast results were achieved at Los Tilos weather station, displaying a better performance for all statistical indicators. Although this station is located further north, and has a lower ET_{ref} values than the others, the percentage indicator $NRMSE$ reveal better performance: the 7-day average of $NRMSE$ in single-day ET^f_{oHS} forecasts is 16.1 %, while the $NRMSE$ of the one-week cumulative ET^f_{oHS} forecast is 11.0 %. The 7-day average of $Accuracy$, $RMSE$, MBE, $NMBE$ and R^2 in the single-day ET^f_{oHS} predictions are 91.8 %, 0.59 $mm\,d^{-1}$, 0.11 $mm\,d^{-1}$, 3.0 % and 0.76, respectively. For the one-week cumulative ET^f_{oHS} forecast values of $RMSE$, MBE, $NMBE$ and R^2 are 2.86 mm, 0.75 mm, 2.9 % and 0.87, respectively.

In the case of El Tambo weather station, the results obtained with HS equation are slightly inferior than those derived using the standardized PM equation, in terms of the indicators $Accuracy$, $RMSE$, $NRMSE$ and R^2, which have 7-day averages in the single-day ET^f_{oHS} forecasts of 72.8 %, 0.98 $mm\,d^{-1}$, 22.3 % and 0.69, respectively; the one week cumulative ET^f_{oHS} forecast yields values of $RMSE$, $NRMSE$ and R^2 are 5.08 mm, 16.3 % and 0.83, respectively. On the other hand, the indicators MBE and $NMBE$ for this

station show less overestimation of ET^f_{oHS} forecasts, with 7-day averages of 0.36 $mm\,d^{-1}$ and 8.3 % in the single-day predictions, and 2.57 mm and 8.3 % for one-week cumulative forecasts.

It is interesting to note that by averaging the $Accuracy$ indicator for single-day ET^f_{oHS} in Table 3.3, for the four weather stations a result of 80.9 % is obtained; i.e., for the whole set of forecasts between 1 and 7 days, on average 80.9 % of the times ET^f_{oHS} is predicted with 1 $mm\,d^{-1}$ or less error. Also, dividing by seven days the $RMSE$ values for one-week cumulative forecasts in each weather station yield 0.51 $mm\,d^{-1}$ at Santa Rosa, 0.55 $mm\,d^{-1}$ at San Clemente, 0.73 $mm\,d^{-1}$ at El Tambo and 0.41 $mm\,d^{-1}$ at Los Tilos. Then, a weekly irrigation schedule based on the $RMSE$ indicator for cumulative ET^f_{oHS} forecasts, on average, could be exceeded by 0.55 $mm\,d^{-1}$. These results point out a satisfactory scenario, and in practice, they could lead to enhancing irrigation management practices in the region.

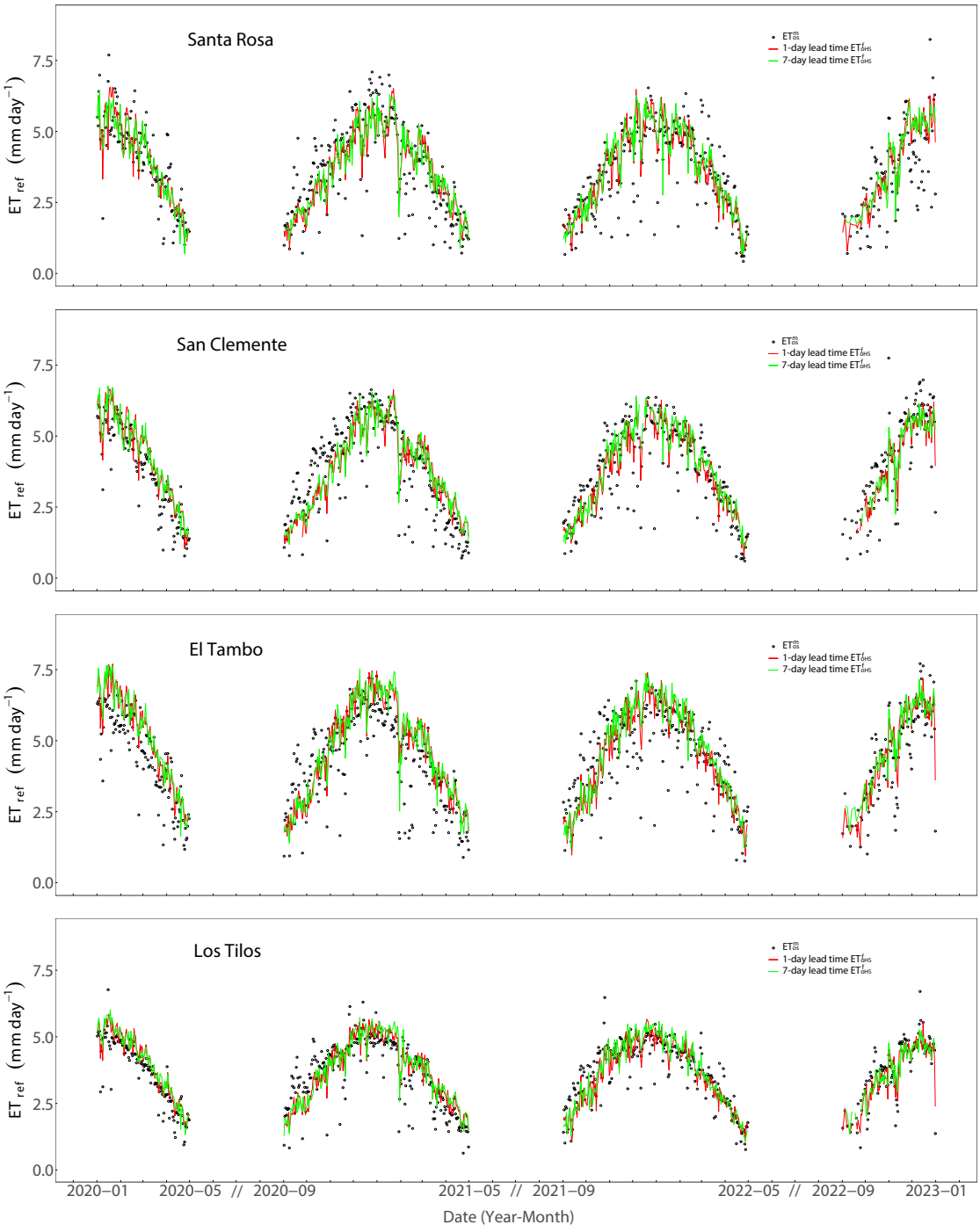

Figure 3.6: Forecasted daily reference evapotranspiration using the Hargreaves-Samani method from Global Forecast System 1 and 7-day ahead temperature predictions (ET^{f}_{oHS}) and the standardized ASCE method from measured weather variables (ET^{m}_{os}), for Santa Rosa, San Clemente, El Tambo and Los Tilos weather stations along the irrigation season (September through April) for the period of 2020 through 2022.

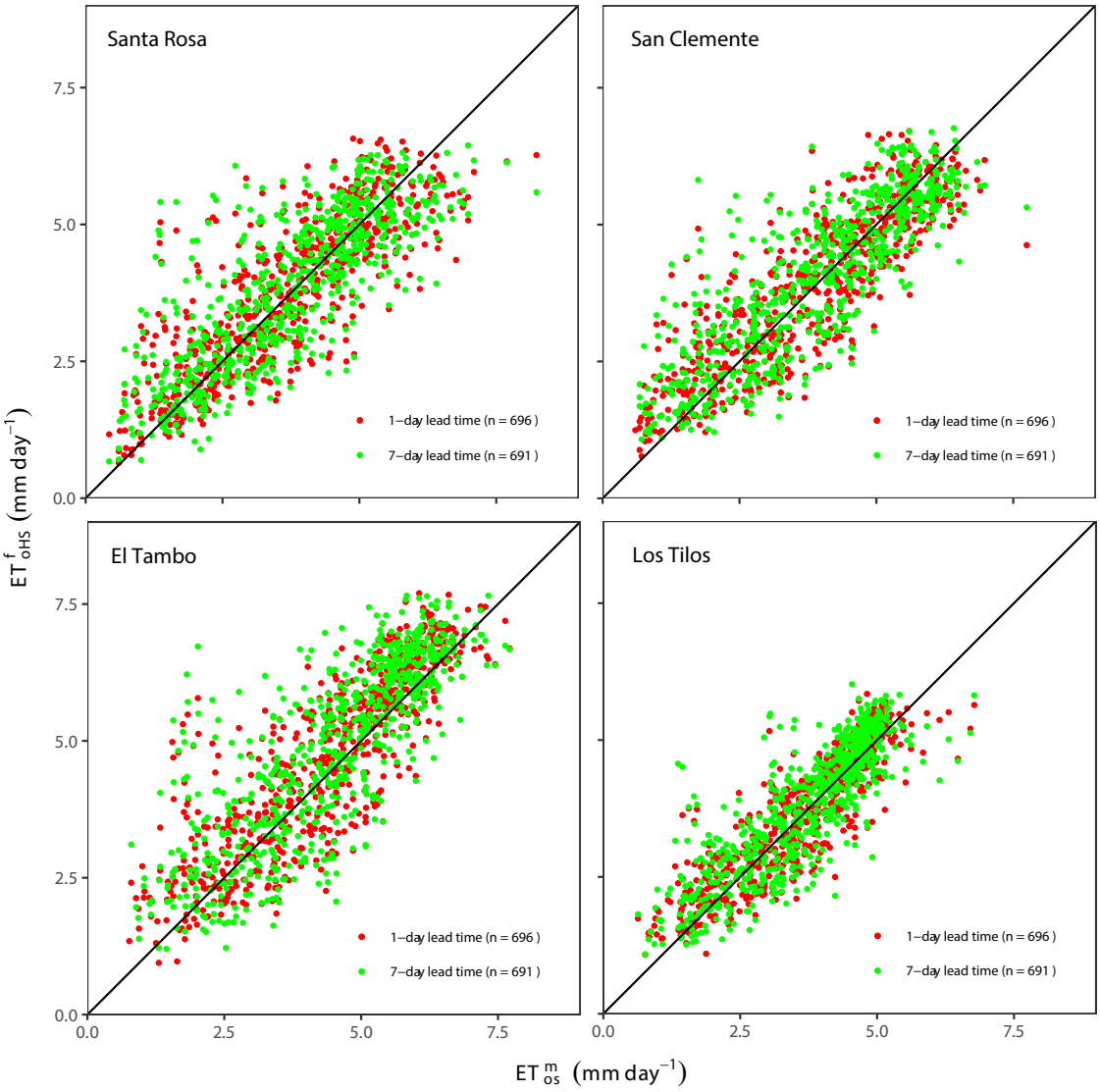

Figure 3.7: 1:1 ratio of forecasted daily reference evapotranspiration using the Hargreaves-Samani method from Global Forecast System 1 and 7-day ahead temperature predictions (ET^{f}_{oHS}) and the standardized ASCE method from measured weather variables (ET^{m}_{os}), for Santa Rosa, San Clemente, El Tambo, and Los Tilos weather stations along the irrigation season (September through April) for the period of 2020 through 2022.

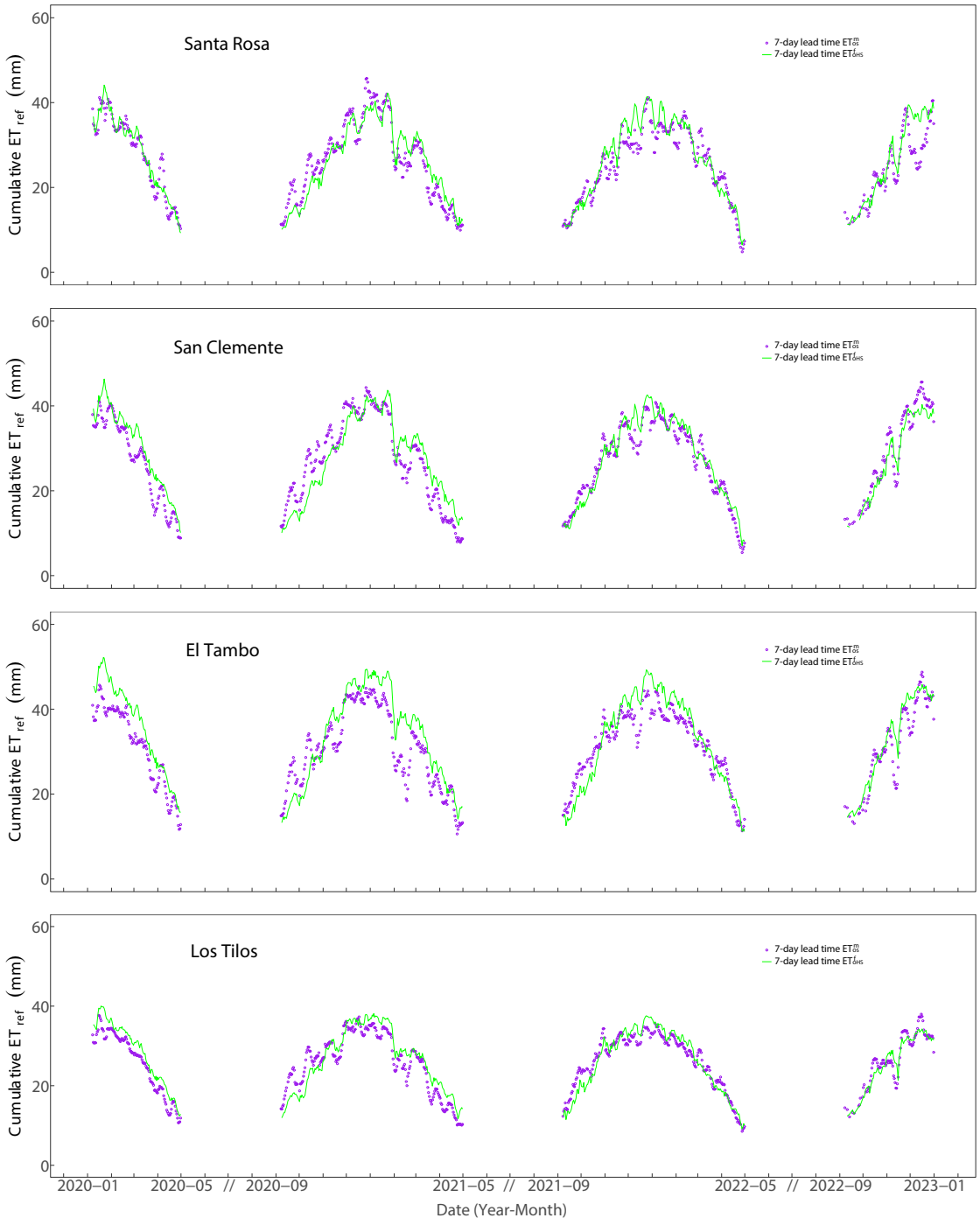

Figure 3.8: Forecasted cumulative 7-day reference evapotranspiration using the Hargreaves-Samani method from Global Forecast System 7-day ahead temperature predictions (ET^f_{oHS}) and standardized ASCE method from measured weather variables (ET^m_{os}), for Santa Rosa, San Clemente, El Tambo and Los Tilos weather stations along the irrigation season (September through April) for the period of 2020 through 2022.

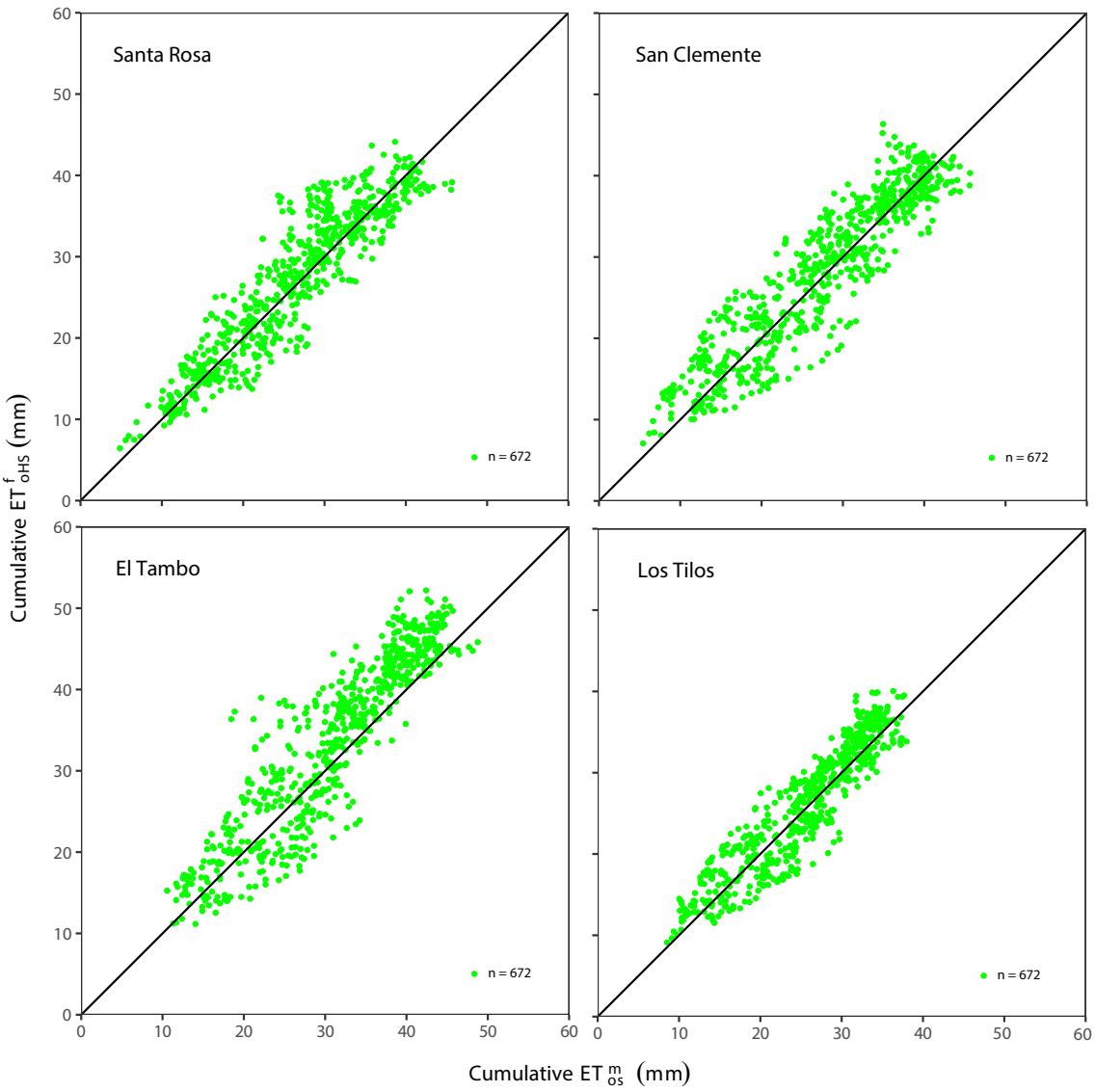

Figure 3.9: 1:1 ratio of forecasted cumulative 7-day reference evapotranspiration using the Hargreaves-Samani method from Global Forecast System 7-day ahead temperature predictions (ET^{f}_{oHS}) and the standardized ASCE method from measured weather variables (ET^{m}_{os}), for Santa Rosa, San Clemente, El Tambo, and Los Tilos weather stations along the irrigation season (September through April) for the period of 2020 through 2022.

Table 3.3: Statistical indices of forecasted daily evapotranspiration using the Hargreaves-Samani method from Global Forecast System 1 to 7-day ahead temperature predictions (ET^{f}_{oHS}) compared with values obtained using the standardized ASCE method from measured weather variables (ET^{m}_{os}), for Santa Rosa, San Clemente, El Tambo and Los Tilos weather stations along the irrigation season (September through April) for the period of 2020 through 2022.

Santa Rosa						
Day of forecast	$Accuracy$ (%)	$RMSE$ (mm d^{-1})	$NRMSE$ (%)	MBE (mm d^{-1})	$NMBE$ (%)	R^2
1	79.7	0.85	23.0	0.09	2.3	0.69
2	78.3	0.87	23.4	0.10	2.8	0.68
3	78.0	0.87	23.3	0.10	2.7	0.68
4	78.7	0.89	24.1	0.11	3.1	0.67
5	78.9	0.91	24.7	0.12	3.3	0.65
6	78.5	0.93	25.0	0.13	3.5	0.64
7	78.2	0.93	25.2	0.11	3.0	0.63
Average	78.6	0.89	24.1	0.11	3.0	0.66

San Clemente						
Day of forecast	$Accuracy$ (%)	$RMSE$ (mm d^{-1})	$NRMSE$ (%)	MBE (mm d^{-1})	$NMBE$ (%)	R^2
1	82.5	0.78	20.0	0.06	1.5	0.76
2	80.7	0.81	20.8	0.08	2.1	0.74
3	81.0	0.80	20.6	0.08	2.0	0.74
4	80.6	0.83	21.3	0.09	2.4	0.73
5	80.4	0.85	21.8	0.10	2.6	0.72
6	78.5	0.87	22.4	0.14	3.7	0.71
7	79.0	0.87	22.3	0.13	3.4	0.70
Average	80.4	0.83	21.3	0.10	2.5	0.73

El Tambo						
Day of forecast	$Accuracy$ (%)	$RMSE$ (mm d^{-1})	$NRMSE$ (%)	MBE (mm d^{-1})	$NMBE$ (%)	R^2
1	75.6	0.91	20.6	0.32	7.2	0.73
2	74.0	0.96	21.7	0.36	8.1	0.70
3	73.9	0.94	21.4	0.35	7.8	0.71
4	72.8	0.97	22.2	0.35	8.0	0.69
5	72.4	1.00	22.8	0.37	8.3	0.68
6	71.8	1.03	23.5	0.41	9.4	0.67
7	69.3	1.05	23.9	0.39	8.9	0.65
Average	72.8	0.98	22.3	0.36	8.3	0.69

Los Tilos						
Day of forecast	$Accuracy$ (%)	$RMSE$ (mm d^{-1})	$NRMSE$ (%)	MBE (mm d^{-1})	$NMBE$ (%)	R^2
1	93.5	0.53	14.4	0.07	2.0	0.81
2	93.1	0.56	15.1	0.10	2.7	0.79
3	93.2	0.57	15.4	0.11	2.9	0.78
4	92.2	0.59	16.0	0.11	3.0	0.77
5	90.6	0.61	16.6	0.12	3.2	0.75
6	89.9	0.63	17.3	0.13	3.5	0.74
7	90.2	0.66	17.8	0.13	3.6	0.72
Average	91.8	0.59	16.1	0.11	3.0	0.76

$RMSE$: Root mean square error; $NRMSE$: Normalized root mean square error; MBE : Mean bias error; $NMBE$: Normalized mean bias error; R^2 : Coefficient of determination.

Table 3.4: Statistical indices of forecasted cumulative 1 to 7-day reference evapotranspiration using the Hargreaves method from Global Forecast System 1 to 7-day ahead temperature predictions (ET^{f}_{oHS}) compared with values obtained using the standardized ASCE method from measured weather variables (ET^{m}_{os}), for Santa Rosa, San Clemente, El Tambo and Los Tilos weather stations along the irrigation season (September through April) for the period of 2020 through 2022.

Santa Rosa					
Day of forecast	$RMSE$ (mm)	$NRMSE$ (%)	MBE (mm)	$NMBE$ (%)	R^2
1	0.85	23.0	0.09	2.3	0.69
2	1.46	19.7	0.19	2.5	0.75
3	1.95	17.5	0.28	2.5	0.79
4	2.39	16.1	0.39	2.6	0.81
5	2.81	15.1	0.52	2.8	0.83
6	3.22	14.4	0.66	2.9	0.84
7	3.60	13.8	0.77	3.0	0.85

San Clemente					
Day of forecast	$RMSE$ (mm)	$NRMSE$ (%)	MBE (mm)	$NMBE$ (%)	R^2
1	0.78	20.0	0.06	1.5	0.76
2	1.39	17.8	0.14	1.7	0.79
3	1.92	16.4	0.21	1.8	0.81
4	2.42	15.5	0.30	1.9	0.83
5	2.91	14.9	0.40	2.0	0.84
6	3.39	14.4	0.53	2.3	0.84
7	3.86	14.0	0.66	2.4	0.85

El Tambo					
Day of forecast	$RMSE$ (mm)	$NRMSE$ (%)	MBE (mm)	$NMBE$ (%)	R^2
1	0.91	20.6	0.32	7.2	0.73
2	1.69	19.2	0.67	7.7	0.76
3	2.40	18.1	1.02	7.7	0.78
4	3.07	17.3	1.38	7.8	0.80
5	3.73	16.8	1.75	7.9	0.82
6	4.41	16.6	2.17	8.1	0.83
7	5.08	16.3	2.57	8.3	0.83

Los Tilos					
Day of forecast	$RMSE$ (mm)	$NRMSE$ (%)	MBE (mm)	$NMBE$ (%)	R^2
1	0.53	14.4	0.07	2.0	0.81
2	0.95	13.0	0.17	2.3	0.83
3	1.36	12.3	0.27	2.5	0.84
4	1.74	11.8	0.38	2.6	0.85
5	2.11	11.4	0.49	2.7	0.86
6	2.48	11.2	0.62	2.8	0.87
7	2.86	11.0	0.75	2.9	0.87

$RMSE$: Root mean square error; $NRMSE$: Normalized root mean square error; MBE : Mean bias error; $NMBE$: Normalized mean bias error; R^2 : Coefficient of determination.

Since the topic of ET forecasting has not yet been widely investigated in Chile, the results presented here may be interesting for farmers, water resource planners and managers, irrigation practitioners, and researchers in the area. Silva et al. (2010) provided ET_{ref} predictions for Central Chile (Maipo river basin) using numerical weather forecasts from the MM5 model (short for Fifth-Generation Penn State/NCAR Mesoscale Model), with three procedures: (a) raw MM5 estimates of latent heat flux; (b) calculation of ET_{ref} from PM equation, using raw MM5 outputs of weather variables; and (c) calculation of ET_{ref} from PM using MOS-corrected (Model Output Statistics) MM5 weather data. In terms of the $RMSE$ index, the results corresponding to the third procedure were the best, obtaining for 1-day-ahead ET_{ref} forecasts values in the range 0.63 to 1.22 $mm\,d^{-1}$, thus similar to the range 0.53 to 0.91 $mm\,d^{-1}$ observed in the present research study.

Moreover, the results obtained in the present study closely align with findings from recent work that makes use of similar weather prediction methodologies to forecast ET_{ref}. In a study conducted in China (Yang et al. 2019b), six ET_{ref} equations were evaluated for 1 to 7 day ahead across various climatic regions. In that research, the authors evaluated five temperature based ET_{ref} models equations (and one combination equation), resembling our approach of utilizing the HS equation and GFS model. Among the six models evaluated, two modified versions of the FAO56-PM equation (Allen et al. 1998) yielded the best ET_{ref} forecasts, followed by the results derived from the HS model. When using the $RMSE$ indicator to compare results, their most accurate ET_{ref} estimations, ranging approximately between 0.7 and 1.1 $mm\,d^{-1}$, are comparable in magnitude to the present outcomes.

Again, in terms of $RMSE$, our results are similar to those presented in others studies also conducted in China (Yang et al. 2016, 2019a), where ET_{ref} is predicted for the 1- to 7-day lead times. In these papers, the authors used modifications of the PM model for short-term ET_{ref} forecasting with temperature data derived from public weather forecasts

and wind speed data, obtaining better results than those achieved with more complex models. In Yang et al. (2016), $RMSE$ ranges between 0.65 and 1.06 $mm\,d^{-1}$, while in Yang et al. (2019a), $RMSE$ ranges approximately between 0.9 and 1.1 $mm\,d^{-1}$. Note that Yang et al. (2016) also use the $Accuracy$ indicator; however, it is not appropriate to compare their results with ours, as we have defined this indicator in a different fashion.

Ben Hamouda et al. (2022) compared FRET (Forecast Reference Evapotranspiration) ET_{ref} predictions with CIMIS (California Irrigation Management Information System) ET_{ref} observed values for various microclimate regions in California, USA. That research work is particularly relevant given it evaluates ET_{ref} forecasts for conditions similar to those of the Central Valley of Chile. Firstly, it assesses forecasts from June to September, which are dates belonging to the irrigation season. Secondly, it includes stations in Warm-summer Mediterranean climate (Csb). Under these climate conditions, the statistical indicators of the 1 to 7-day FRET ET_{ref} forecasts fall within a comparable range to those of the present research; in particular, $RMSE$ indicator, ranging between 0.54 to 0.99 $mm\,d^{-1}$, show results comparable to the present study.

Overall, the numbers obtained and the consistency of the results between these studies and the present study suggest the effectiveness of using weather forecasts to predict ET_{ref} and their potential applicability in the context of more precise irrigation management.

3.4 Conclusions

In this work, 1- to 7-day ET_{ref} forecasts were evaluated for the Mediterranean climate of Central Chile. The evaluation used weather data measured at four automated weather stations and predicted by the GFS model over the course of irrigation seasons of 2020-2022. ET_{ref} forecasts from the ASCE standardized PM equation and the HS equation, using predicted weather data, were compared with ET_{ref} values calculated from measured

data using the ASCE standardized PM equation. The forecasts were assessed through time series analysis, 1:1 plots, and various statistical indicators.

The single-day and cumulative ET_{os}^{f} predictions for a short canopy crop, based on the GFS forecasts of incident solar radiation, air temperature, relative humidity, and wind speed, using the ASCE calculation procedure, evidenced a significant overestimation of ET_{os}^{f}, with 7-day average of $NMBE$ ranging from 9.1 to 36.9 %. This overestimation can be explained with the combined effects of underestimation of relative humidity predictions and overestimation of incoming solar radiation and wind speed predictions.

However, when ET_{ref} predictions were based only on GFS temperature forecasts (which showed a better performance compared to the remaining three meteorological variables), and using the HS equation, the results were significantly improved.

For the four weather stations, the 7-day average of statistical indices of single-day ET_{oHS}^{f} predictions based on GFS air temperature encompass within the following ranges: $Accuracy$: 72.8 to 91.8 %; $RMSE$: 0.59 to 0.98 $mm\,d^{-1}$; $NRMSE$: 16.1 to 24.1 %; MBE: 0.10 to 0.36 $mm\,d^{-1}$; $NMBE$: 2.5 to 8.3 %. For the four-station average, the $Accuracy$ index shows that 80.9 % of the times the ET_{oHS}^{f} forecasts missed by 1 $mm\,d^{-1}$ or less.

On the other hand, the indicators for the 1-week cumulative ET_{oHS}^{f} forecasts falls within the ranges: $RMSE$: 2.86 to 5.08 mm; $NRMSE$: 11.0 to 16.3 %; MBE: 0.66 to 2.57 mm; $NMBE$: 2.4 to 8.3 %. When the four station average of cumulative ET_{oHS}^{f} $RMSE$ value is divided by 7 days, an overestimation of 0.55 $mm\,d^{-1}$ for a 1-week-ahead irrigation schedule is obtained.

These results align with recent research using similar methods to forecast ET_{ref} based on weather predictions. Thus, 1-day to 7-day GFS weather data predictions allow to generate ET_{ref} forecasts with the potential to estimate appropriately near-time crop water demand in Central Chile. In practice, forecasts of this nature could be particularly useful

for irrigation scheduling, especially in high-frequency water application systems.

Finally, it is important to note that the ET_{ref} estimation method used, based only on air temperature, as an alternative to the ASCE's first option procedure was selected to achieve the best forecast results within a common framework for all four weather stations. It is likely that better results could be obtained by implementing tailored procedures for each station individually. Although this research was carried out in Chile, the GFS model has a global scope, and ET_{ref} forecasts can be obtained for any location worldwide. Future research could explore forecasting and assessing ET_{ref} in other regions of interest, incorporating site-specific adjustments and corrections to pursue more accurate water demand predictions.

Acknowledgements

This research has been partially funded by Centro de Recursos Hídricos para la Agricultura y la Minería CRHIAM, ANID/FONDAP/15130015 and ANID/FONDAP/1523A0001, the project Chileflux: a scientific network for monitoring water, energy and CO2 fluxes as a tool for the control, adaptation and mitigation of climate change and drought in Chile" ANID/FSEQ210019 and the Consorcio Tecnológico del Agua CoTH2O CORFO/20CTECGH145896.

A Appendix. Monthly averages and statistical indicators for weather variables

Assessing the forecasts of the meteorological variables involved in the ET process is essential for understanding the forecast behavior. In this appendix, the monthly averages of these variables, along with the corresponding values of the considered statistical indicators, are summarized.

Fig. 3.10 to 3.13 present the monthly average values of weather variables daily maximum and minimum air temperatures, incoming solar radiation, mean relative humidity, and mean wind speed, for stations Santa Rosa, San Clemente, El Tambo, and Los Tilos. These figures show data from the irrigation seasons spanning September to April across the three-year period from 2020 to 2022.

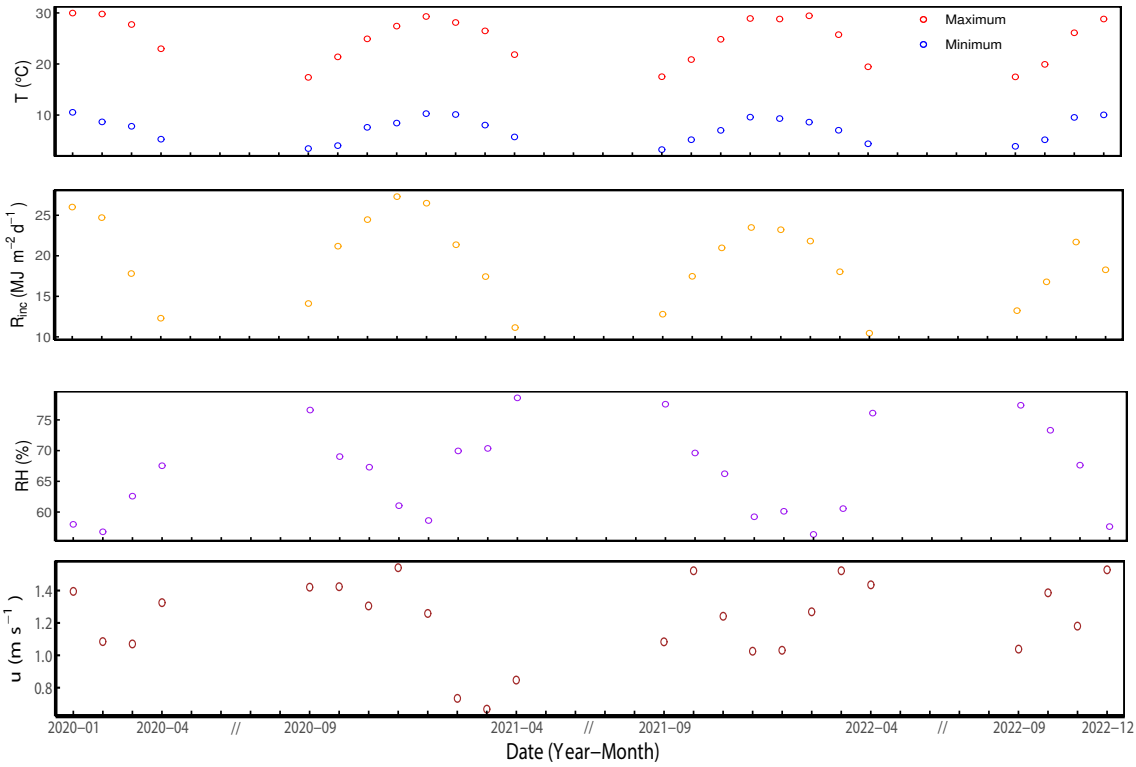

Figure 3.10: Monthly averages of daily maximum and minimum air temperature (T), incoming solar radiation (R_{inc}), mean relative humidity (RH), and mean wind speed (u) for Santa Rosa weather station along the irrigation season (September through April) for the period of 2020 through 2022.

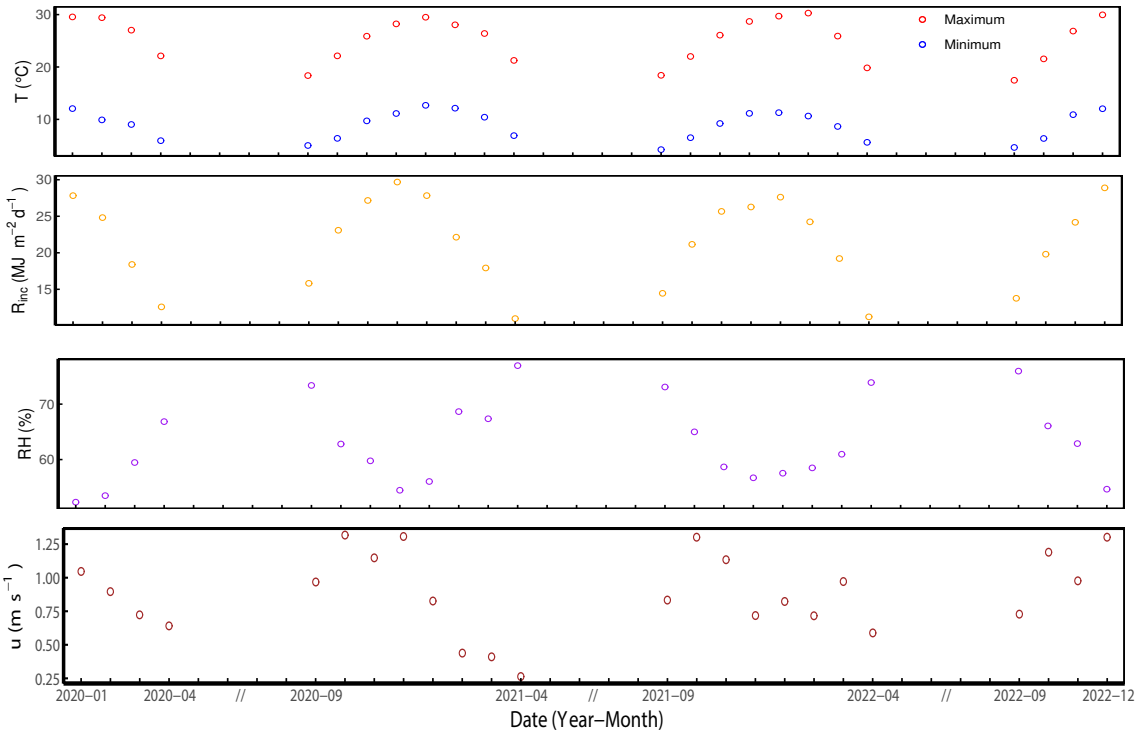

Figure 3.11: Monthly averages of daily maximum and minimum air temperature (T), incoming solar radiation (R_{inc}), mean relative humidity (RH), and mean wind speed (u) for San Clemente weather station along the irrigation season (September through April) for the period of 2020 through 2022.

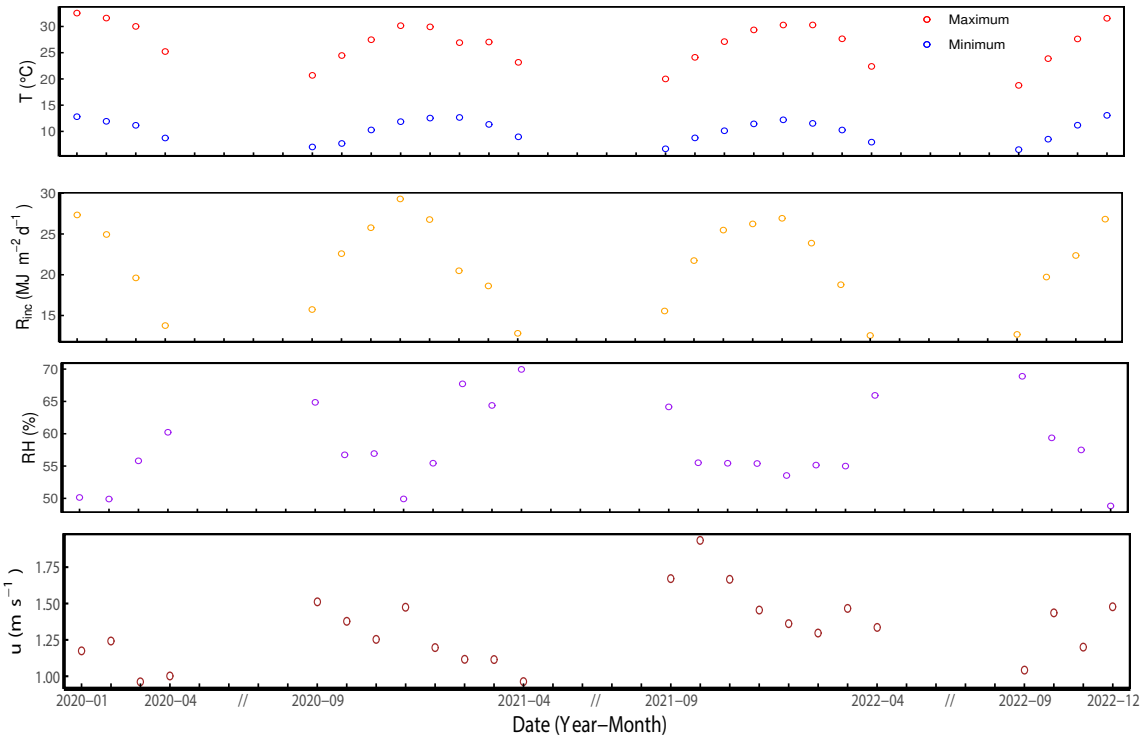

Figure 3.12: Monthly averages of daily maximum and minimum air temperature (T), incoming solar radiation (R_{inc}), mean relative humidity (RH), and mean wind speed (u) for El Tambo weather station along the irrigation season (September through April) for the period of 2020 through 2022.

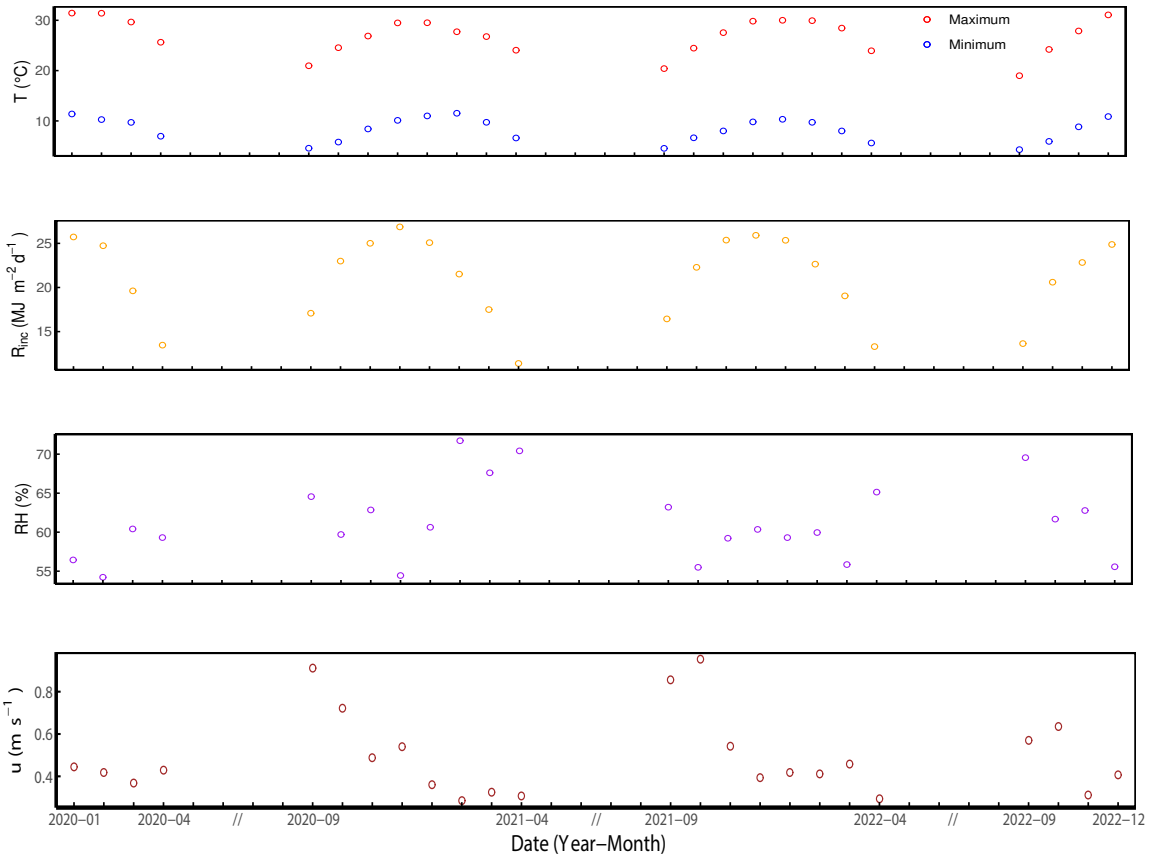

Figure 3.13: Monthly averages of daily maximum and minimum air temperature (T), incoming solar radiation (R_{inc}), mean relative humidity (RH), and mean wind speed (u) for Los Tilos weather station along the irrigation season (September through April) for the period of 2020 through 2022.

For the same time period and the four weather stations, the statistical indicators $RMSE$, $NRMSE$, MBE, $NMBE$ and R^2 for 1 to 7-day GFS forecast of maximum, minimum and mean daily temperature, daily incoming solar radiation, mean daily relative humidity and mean daily wind speed, are shown in Tables 3.5 to 3.8.

Table 3.5: Statistical indices of the Global Forecast System forecast of maximum, minimum and mean daily temperature, daily incoming solar radiation, mean daily relative humidity, and mean daily wind speed, for Santa Rosa weather station, corresponding to 1-to-7-day predictions, with their averages, along the irrigation season (September through April) for the period of 2020 through 2022.

Maximum daily temperature					
Day of forecast	$RMSE$ ($^{\circ}C$)	$NRMSE$ (%)	MBE ($^{\circ}C$)	$NMBE$ (%)	R^2
1	3.3	13.2	2.2	8.9	0.87
2	3.5	14.0	2.4	9.6	0.86
3	3.6	14.2	2.4	9.5	0.84
4	3.7	14.8	2.4	9.7	0.82
5	3.9	15.5	2.5	9.9	0.79
6	4.2	16.8	2.6	10.4	0.75
7	4.3	17.3	2.5	10.1	0.71
Average	3.8	15.1	2.4	9.7	0.81

Minimum daily temperature					
Day of forecast	$RMSE$ ($^{\circ}C$)	$NRMSE$ (%)	MBE ($^{\circ}C$)	$NMBE$ (%)	R^2
1	2.3	32.0	1.1	14.7	0.65
2	2.5	33.5	1.2	15.9	0.62
3	2.6	34.9	1.2	16.7	0.59
4	2.6	35.3	1.2	16.2	0.57
5	2.6	35.8	1.1	15.0	0.54
6	2.9	39.2	1.3	18.1	0.49
7	3.0	40.5	1.3	18.2	0.46
Average	2.6	35.9	1.2	16.4	0.56

Mean daily temperature					
Day of forecast	$RMSE$ ($^{\circ}C$)	$NRMSE$ (%)	MBE ($^{\circ}C$)	$NMBE$ (%)	R^2
1	2.2	13.8	1.7	10.2	0.89
2	2.4	14.8	1.8	11.0	0.88
3	2.5	15.1	1.8	11.1	0.86
4	2.5	15.5	1.8	11.2	0.85
5	2.6	15.8	1.8	11.0	0.83
6	2.8	17.5	2.0	12.1	0.79
7	2.9	17.9	1.9	12.0	0.76
Average	2.6	15.8	1.8	11.2	0.84

Daily incoming solar radiation					
Day of forecast	$RMSE$ (MJ m^{-2} d^{-1})	$NRMSE$ (%)	MBE (MJ m^{-2} d^{-1})	$NMBE$ (%)	R^2
1	8.03	41.4	6.77	34.9	0.67
2	8.16	41.9	6.84	35.1	0.64
3	8.08	41.3	6.72	34.4	0.63
4	8.25	42.4	6.81	35.0	0.62
5	8.51	43.8	6.98	35.9	0.58
6	8.73	44.8	6.88	35.3	0.47
7	8.81	45.2	6.84	35.1	0.44
Average	8.37	43.0	6.83	35.1	0.58

Mean daily relative humidity					
Day of forecast	$RMSE$ (%)	$NRMSE$ (%)	MBE (%)	$NMBE$ (%)	R^2
1	12.2	18.5	-9.2	-13.8	0.68
2	13.1	19.8	-9.7	-14.7	0.61
3	13.6	20.6	-10.1	-15.3	0.58
4	13.9	21.0	-10.3	-15.6	0.56
5	14.4	21.8	-10.6	-16.0	0.53
6	15.0	22.7	-10.8	-16.2	0.46
7	15.4	23.2	-10.8	-16.3	0.42
Average	14.0	21.1	-10.2	-15.4	0.55

Mean daily wind speed					
Day of forecast	$RMSE$ ($m\ s^{-1}$)	$NRMSE$ (%)	MBE ($m\ s^{-1}$)	$NMBE$ (%)	R^2
1	0.53	43.1	0.18	15.0	0.67
2	0.54	44.4	0.18	15.1	0.63
3	0.57	46.6	0.19	15.9	0.58
4	0.60	48.7	0.20	16.0	0.53
5	0.64	52.6	0.22	18.2	0.44
6	0.70	57.3	0.20	16.6	0.32
7	0.76	62.0	0.21	16.9	0.22
Average	0.62	50.7	0.20	16.2	0.49

$RMSE$: Root mean square error; $NRMSE$: Normalized root mean square error; MBE : Mean bias error; $NMBE$: Normalized mean bias error; R^2 : Coefficient of determination.

Table 3.6: Statistical indices of the Global Forecast System forecast of maximum, minimum and mean daily temperature, daily incoming solar radiation, mean daily relative humidity, and mean daily wind speed, for San Clemente weather station, corresponding to 1-to-7-day predictions, with their averages, along the irrigation season (September through April) for the period of 2020 through 2022.

Maximum daily temperature					
Day of forecast	$RMSE$ ($^{\circ}C$)	$NRMSE$ (%)	MBE ($^{\circ}C$)	$NMBE$ (%)	R^2
1	4.0	15.8	2.8	11.1	0.83
2	4.3	16.7	3.0	11.8	0.81
3	4.3	16.9	3.0	11.8	0.80
4	4.4	17.1	3.1	12.0	0.79
5	4.6	17.9	3.1	12.2	0.75
6	4.9	19.2	3.4	13.4	0.74
7	5.0	19.6	3.4	13.3	0.69
Average	4.5	17.6	3.1	12.2	0.77

Minimum daily temperature					
Day of forecast	$RMSE$ ($^{\circ}C$)	$NRMSE$ (%)	MBE ($^{\circ}C$)	$NMBE$ (%)	R^2
1	2.4	26.3	-0.5	-5.1	0.56
2	2.4	26.4	-0.3	-3.2	0.55
3	2.4	27.0	-0.2	-2.5	0.53
4	2.5	27.3	-0.3	-3.3	0.52
5	2.5	28.1	-0.4	-4.3	0.49
6	2.6	28.8	-0.2	-2.1	0.46
7	2.7	30.3	-0.2	-2.2	0.42
Average	2.5	27.8	-0.3	-3.3	0.51

Mean daily temperature					
Day of forecast	$RMSE$ ($^{\circ}C$)	$NRMSE$ (%)	MBE ($^{\circ}C$)	$NMBE$ (%)	R^2
1	2.1	12.1	1.2	6.8	0.85
2	2.2	12.9	1.4	7.9	0.84
3	2.3	13.3	1.4	8.1	0.83
4	2.3	13.4	1.4	8.0	0.82
5	2.4	13.8	1.4	7.8	0.80
6	2.6	15.3	1.6	9.4	0.78
7	2.7	15.6	1.6	9.2	0.75
Average	2.4	13.8	1.4	8.2	0.81

Daily incoming solar radiation					
Day of forecast	$RMSE$ (MJ m^{-2} d^{-1})	$NRMSE$ (%)	MBE (MJ m^{-2} d^{-1})	$NMBE$ (%)	R^2
1	6.02	27.9	5.02	23.2	0.80
2	6.28	28.9	5.08	23.4	0.75
3	6.22	28.5	5.01	23.0	0.75
4	6.47	29.9	5.15	23.8	0.73
5	6.61	30.5	5.07	23.4	0.68
6	6.97	32.7	5.21	24.0	0.62
7	7.04	32.4	5.15	23.7	0.58
Average	6.52	30.0	5.10	23.5	0.70

Mean daily relative humidity					
Day of forecast	$RMSE$ (%)	$NRMSE$ (%)	MBE (%)	$NMBE$ (%)	R^2
1	13.0	20.6	-8.4	-13.4	0.56
2	14.0	22.3	-9.2	-14.6	0.48
3	14.5	23.1	-9.5	-15.2	0.45
4	14.7	23.4	-9.8	-15.6	0.44
5	15.0	23.9	-9.8	-15.6	0.42
6	15.2	24.1	-9.9	-15.8	0.39
7	15.7	25.0	-10.2	-16.3	0.33
Average	14.6	23.2	-9.5	-15.2	0.44

Mean daily wind speed					
Day of forecast	$RMSE$ ($m\ s^{-1}$)	$NRMSE$ (%)	MBE ($m\ s^{-1}$)	$NMBE$ (%)	R^2
1	0.48	53.3	0.23	25.7	0.58
2	0.47	52.9	0.21	23.8	0.55
3	0.49	54.5	0.22	24.2	0.50
4	0.51	57.7	0.23	25.6	0.45
5	0.53	59.1	0.23	26.4	0.40
6	0.55	61.7	0.22	24.5	0.32
7	0.58	64.6	0.22	24.8	0.25
Average	0.52	57.7	0.22	25.0	0.44

$RMSE$: Root mean square error; $NRMSE$: Normalized root mean square error; MBE : Mean bias error; $NMBE$: Normalized mean bias error; R^2 : Coefficient of determination.

Table 3.7: Statistical indices of the Global Forecast System forecast of maximum, minimum and mean daily temperature, daily incoming solar radiation, mean daily relative humidity, and mean daily wind speed, for El Tambo weather station, corresponding to 1-to-7-day predictions, with their averages, along the irrigation season (September through April) for the period of 2020 through 2022.

Maximum daily temperature					
Day of forecast	$RMSE$ ($^{\circ}C$)	$NRMSE$ (%)	MBE ($^{\circ}C$)	$NMBE$ (%)	R^2
1	3.2	11.9	1.4	5.2	0.78
2	3.5	12.8	1.7	6.2	0.74
3	3.5	13.1	1.7	6.2	0.72
4	3.7	13.6	1.7	6.3	0.70
5	3.8	14.2	1.7	6.2	0.67
6	4.0	15.0	2.0	7.2	0.65
7	4.2	15.6	1.9	6.9	0.60
Average	3.7	13.7	1.7	6.3	0.69

Minimum daily temperature					
Day of forecast	$RMSE$ ($^{\circ}C$)	$NRMSE$ (%)	MBE ($^{\circ}C$)	$NMBE$ (%)	R^2
1	2.5	24.4	-0.6	-6.0	0.41
2	2.5	24.5	-0.5	-4.4	0.39
3	2.6	24.9	-0.3	-3.3	0.37
4	2.6	24.8	-0.4	-3.9	0.36
5	2.6	25.5	-0.5	-5.1	0.34
6	2.7	26.1	-0.5	-4.4	0.31
7	2.8	27.1	-0.5	-4.9	0.27
Average	2.6	25.3	-0.5	-4.6	0.35

Mean daily temperature					
Day of forecast	$RMSE$ ($^{\circ}C$)	$NRMSE$ (%)	MBE ($^{\circ}C$)	$NMBE$ (%)	R^2
1	2.0	10.6	0.4	2.1	0.78
2	2.1	11.3	0.6	3.2	0.76
3	2.2	11.7	0.7	3.6	0.74
4	2.2	12.0	0.7	3.5	0.72
5	2.3	12.5	0.6	3.1	0.69
6	2.4	13.1	0.8	4.0	0.67
7	2.6	13.7	0.7	3.6	0.63
Average	2.3	12.1	0.6	3.3	0.71

Daily incoming solar radiation					
Day of forecast	$RMSE$ (MJ m^{-2} d^{-1})	$NRMSE$ (%)	MBE (MJ m^{-2} d^{-1})	$NMBE$ (%)	R^2
1	6.57	30.6	5.67	26.4	0.76
2	6.72	31.2	5.72	26.5	0.73
3	6.51	30.1	5.60	25.9	0.75
4	6.75	31.4	5.72	26.6	0.72
5	6.97	32.4	5.68	26.4	0.67
6	7.26	33.8	5.84	27.2	0.60
7	7.25	33.6	5.72	26.5	0.57
Average	6.86	31.9	5.71	26.5	0.69

Mean daily relative humidity					
Day of forecast	$RMSE$ (%)	$NRMSE$ (%)	MBE (%)	$NMBE$ (%)	R^2
1	13.7	23.6	-7.6	-13.2	0.46
2	14.8	25.6	-8.3	-14.4	0.34
3	15.5	26.8	-8.8	-15.3	0.29
4	15.7	27.1	-9.1	-15.7	0.29
5	16.1	27.9	-9.0	-15.6	0.25
6	16.5	28.5	-9.3	-16.1	0.24
7	16.7	29.0	-9.2	-16.0	0.19
Average	15.6	26.9	-8.8	-15.2	0.29

Mean daily wind speed					
Day of forecast	$RMSE$ ($m\ s^{-1}$)	$NRMSE$ (%)	MBE ($m\ s^{-1}$)	$NMBE$ (%)	R^2
1	0.67	50.4	-0.50	-37.5	0.20
2	0.68	51.3	-0.51	-38.3	0.18
3	0.68	50.9	-0.51	-38.1	0.18
4	0.68	51.0	-0.50	-37.8	0.15
5	0.67	50.9	-0.49	-37.2	0.14
6	0.68	51.0	-0.49	-37.1	0.12
7	0.70	52.4	-0.50	-37.7	0.06
Average	0.68	51.1	-0.50	-37.7	0.15

$RMSE$: Root mean square error; $NRMSE$: Normalized root mean square error; MBE : Mean bias error; $NMBE$: Normalized mean bias error; R^2 : Coefficient of determination.

Table 3.8: Statistical indices of the Global Forecast System forecast of maximum, minimum and mean daily temperature, daily incoming solar radiation, mean daily relative humidity, and mean daily wind speed, for Los Tilos weather station, corresponding to 1-to-7-day predictions, with their averages, along the irrigation season (September through April) for the period of 2020 through 2022.

Maximum daily temperature					
Day of forecast	$RMSE$ ($^{\circ}C$)	$NRMSE$ (%)	MBE ($^{\circ}C$)	$NMBE$ (%)	R^2
1	2.0	7.4	1.0	3.7	0.88
2	2.3	8.5	1.2	4.5	0.84
3	2.5	9.1	1.3	4.7	0.81
4	2.7	9.8	1.3	4.9	0.78
5	2.9	10.6	1.3	4.8	0.74
6	3.2	11.7	1.4	5.0	0.68
7	3.4	12.4	1.4	5.0	0.62
Average	2.7	9.9	1.3	4.7	0.76

Minimum daily temperature					
Day of forecast	$RMSE$ ($^{\circ}C$)	$NRMSE$ (%)	MBE ($^{\circ}C$)	$NMBE$ (%)	R^2
1	4.5	53.4	3.3	38.9	0.26
2	4.7	56.2	3.5	41.3	0.24
3	4.8	57.3	3.6	42.5	0.23
4	4.8	56.9	3.5	41.8	0.21
5	4.8	56.5	3.4	40.5	0.18
6	4.8	56.8	3.3	39.3	0.16
7	4.9	57.7	3.3	39.1	0.14
Average	4.8	56.4	3.4	40.5	0.20

Mean daily temperature					
Day of forecast	$RMSE$ ($^{\circ}C$)	$NRMSE$ (%)	MBE ($^{\circ}C$)	$NMBE$ (%)	R^2
1	2.6	14.7	2.1	12.1	0.84
2	2.9	16.0	2.3	13.2	0.80
3	2.9	16.5	2.4	13.6	0.78
4	3.0	16.9	2.4	13.6	0.75
5	3.0	17.1	2.4	13.3	0.71
6	3.2	17.8	2.3	13.2	0.66
7	3.3	18.2	2.3	13.1	0.61
Average	3.0	16.8	2.3	13.1	0.74

Daily incoming solar radiation					
Day of forecast	$RMSE$ (MJ m^{-2} d^{-1})	$NRMSE$ (%)	MBE (MJ m^{-2} d^{-1})	$NMBE$ (%)	R^2
1	7.08	33.5	6.50	30.8	0.80
2	7.11	33.5	6.44	30.4	0.77
3	7.13	33.5	6.48	30.5	0.77
4	7.29	34.4	6.54	30.9	0.73
5	7.33	34.6	6.47	30.6	0.71
6	7.61	35.9	6.60	31.1	0.62
7	7.65	36.0	6.53	30.8	0.58
Average	7.31	34.5	6.51	30.7	0.71

Mean daily relative humidity					
Day of forecast	$RMSE$ (%)	$NRMSE$ (%)	MBE (%)	$NMBE$ (%)	R^2
1	15.8	25.8	-12.7	-20.8	0.58
2	17.2	28.2	-13.6	-22.3	0.44
3	18.0	29.7	-14.2	-23.3	0.36
4	18.5	30.3	-14.5	-23.8	0.34
5	18.8	30.8	-14.6	-23.8	0.30
6	19.5	31.8	-14.9	-24.4	0.26
7	19.5	32.1	-14.8	-24.3	0.21
Average	18.2	29.8	-14.2	-23.3	0.36

Mean daily wind speed					
Day of forecast	$RMSE$ ($m\ s^{-1}$)	$NRMSE$ (%)	MBE ($m\ s^{-1}$)	$NMBE$ (%)	R^2
1	0.49	99.8	0.30	60.0	0.03
2	0.49	99.6	0.30	60.2	0.02
3	0.49	100.7	0.30	61.7	0.04
4	0.50	102.2	0.31	62.8	0.04
5	0.49	100.4	0.31	63.3	0.01
6	0.50	101.7	0.31	62.7	0.03
7	0.49	100.4	0.30	61.8	0.02
Average	0.49	100.7	0.30	61.8	0.03

$RMSE$: Root mean square error; $NRMSE$: Normalized root mean square error; MBE : Mean bias error; $NMBE$: Normalized mean bias error; R^2 : Coefficient of determination.

CHAPTER 4

CONCLUSIONES

En el manuscrito *Forecasting Reference Evapotranspiration in the Mediterranean Climate of Central Chile using the ASCE Standardized Penman-Monteith Equation, the Hargreaves-Samani Equation, and Weather Predictions of the Global Forecast System Model*, presentado casi en su totalidad en el Capítulo 3, se evaluaron los pronósticos diarios y acumulados de ET_{ref} para cuatro estaciones meteorológicas durante las temporadas de riego entre 2020 y 2022, dentro del horizonte de pronóstico de 1 a 7 días. Aunque las principales conclusiones de la investigación ya se presentaron en la Sección 3.4, es conveniente añadir los siguientes puntos en relación con las hipótesis y objetivos planteados:

1. El objetivo general (OG) de esta tesis, que consistía en evaluar los pronósticos de ET_{ref} obtenidos a partir de las predicciones del GFS de variables meteorológicas, se logró satisfactoriamente. Aunque los pronósticos de ET_{ref} obtenidos inicialmente utilizando la ecuación PM estandarizada de ASCE, derivados de las predicciones del GFS de las variables meteorológicas temperatura del aire, radiación solar incidente, humedad relativa y velocidad del viento, mostraron un rendimiento moderado, los resultados obtenidos utilizando el modelo HS y las predicciones de temperatura del GFS fueron superiores, lo que respalda la hipótesis (H) de este trabajo. Es decir,

las predicciones diarias de ET_{ref} muestran promedios de 7 días en el indicador $Exactitud$ cercanos al 80 %: Santa Rosa: 78.6 %; San Clemente: 80.4 %; El Tambo: 72.8 %; Los Tilos: 91.8 % (Tabla 3.3).

2. Se analizó la pertinencia de varias estaciones meteorológicas de la red Agrometeorología en la Zona Central de Chile (OE1), y se seleccionaron las de Santa Rosa, San Clemente, El Tambo y Los Tilos para esta investigación (Subsec. 3.2.6), debido a su ubicación y al hecho de que presentaron datos de buena calidad durante el período 2020-2022. Estas cuatro estaciones meteorológicas están situadas en distritos agroclimáticos con clima mediterráneo, Csb según la clasificación de Köppen.

3. Se compararon los datos meteorológicos de las cuatro variables en la ecuación PM, considerando los valores medidos en las cuatro estaciones meteorológicas y los datos pronosticados por el modelo GFS en el píxel correspondiente (OE2). Las predicciones de temperatura exhibieron el mejor rendimiento, mientras que las predicciones para la radiación solar incidente y la velocidad del viento fueron sobreestimadas, y la humedad relativa fue subestimada (Tablas 3.5 a 3.8). Consecuentemente, esto condujo a una sobreestimación de los pronósticos de ET_{ref} cuando se obtuvieron utilizando la ecuación PM estandarizada de la ASCE (Subsec. 3.3.1). Este análisis permitió prever el rendimiento superior del modelo HS en los pronósticos de ET_{ref}, ya que estos se basan únicamente en las temperaturas máximas y mínimas diarias como datos de entrada (Subsec. 3.3.2).

4. Los pronósticos diarios y acumulativos de ET_{ref} se evaluaron utilizando series temporales (Figs. 3.2, 3.4, 3.6, y 3.8), gráficos 1:1 (Figs. 3.3, 3.5, 3.7, y 3.9) y los indicadores estadísticos $Accuracy$, $RMSE$, $NRMSE$, MBE, $NMBE$, and R^2 (Tables 3.1, 3.2, 3.3 y 3.4) (OE3). Consistente con lo mencionado anteriormente,

las series temporales y los gráficos 1:1 correspondientes a las predicciones de ET_{ref} basadas en la ecuación PM estandarizada de ASCE mostraron una clara sobreestimación (Figs. 3.2, 3.3, 3.4, y 3.5). En contraste, los pronósticos de ET_{ref} basados en la ecuación HS demostraron un ajuste superior (Figs. 3.6, 3.7, 3.8, y 3.9). Esta mejora también se evidencia en los indicadores estadísticos, con valores promedio de 7 días para las predicciones diarias del HS en los rangos (excluyendo el indicador $Exactitud$, que ya fue proporcionado recientemente): $RMSE$: 0.59-0.98 $mm\,d^{-1}$; $NRMSE$: 16.1-24.1 %; MBE: 0.10-0.36 $1\,mm\,d^{-1}$; $NMBE$: 2.5-8.3 %; y R^2: 0.66-0.76.

Los resultados obtenidos sugieren la efectividad y el potencial de los pronósticos meteorológicos del GFS como base para predecir ET en un futuro cercano, lo que podría impactar positivamente la gestión del agua en la agricultura, especialmente en la programación del riego. Estos hallazgos podrían ser relevantes para agricultores e investigadores en Chile, ya que el tema de los pronósticos de ET aún no se ha desarrollado ampliamente en el país. Posiblemente, la implementación de ajustes locales en el proceso de predicción de ET podría mejorar la precisión de los pronósticos y beneficiar la gestión del riego no solo en Chile, sino también en otras regiones, dado el alcance global del modelo GFS. Finalmente, estas consideraciones podrían guiar investigaciones futuras en este campo.

CHAPTER 5

CONCLUSIONS

In the manuscript *Forecasting Reference Evapotranspiration in the Mediterranean Climate of Central Chile using the ASCE Standardized Penman-Monteith Equation, the Hargreaves-Samani Equation, and Weather Predictions of the Global Forecast System Model*, presented almost entirely in Chapter 3, daily and cumulative ET_{ref} forecasts were evaluated for four weather stations during the irrigation seasons between 2020 and 2022, within the 1-7 day forecast horizon. Although the main conclusions of the research have already been presented in Sec. 3.4, it is convenient to add the following points regarding the hypotheses and objectives outlined:

1. The general objective (GO) of this thesis, consisting of evaluating ET_{ref} forecasts obtained from GFS predictions of meteorological variables, was satisfactorily achieved. Although the ET_{ref} forecasts initially obtained using the ASCE standardized PM equation, derived from GFS predictions of weather variables air temperature, incoming solar radiation, relative humidity and wind speed, showed a moderate performance, the results obtained from using the HS model and GFS temperature predictions were superior, and they support hypothesis (H) of this work. That is, daily ET_{ref} predictions exhibit 7-day averages in the $Accuracy$ indicator close to 80 %: Santa Rosa: 78.6 %; San Clemente: 80.4 %; El Tambo: 72.8 %; Los

Tilos: 91.8 % (Table 3.3).

2. The pertinence of several weather stations of the Agrometeorología network in the Central Zone of Chile was analyzed (EO1), and those of Santa Rosa, San Clemente, El Tambo and Los Tilos were selected for this research (Subsec. 3.2.6), due to their location and the fact that they presented good quality data during the period 2020-2022. These four weather stations are located in agroclimatic districts with Mediterranean climate, Csb according to the Köppen classification.

3. The weather data for the four variables in the PM equation were compared across the four stations with the forecasted data from the GFS model for the corresponding pixel (EO2). Temperature predictions exhibited the best performance, whereas GFS forecasts for incident solar radiation and wind speed were overestimated, and relative humidity was underestimated (Tables 3.5 to 3.8). Consequently, this led to an overestimation of ET_{ref} forecasts when obtained using the standardized PM equation of the ASCE (Subsec. 3.3.1). This analysis provided insights into the superior performance of the HS model in ET_{ref} forecasts, which relies solely on daily maximum and minimum temperatures as input data (Subsec. 3.3.2).

4. The daily and cumulative ET_{ref} forecasts were evaluated using time series (Figs. 3.2, 3.4, 3.6, and 3.8), 1:1 plots (Figs. 3.3, 3.5, 3.7, and 3.9) and the statistical indicators $Accuracy$, $RMSE$, $NRMSE$, MBE, $NMBE$, and R^2 (Tables 3.1, 3.2, 3.3 and 3.4) (EO3). Consistent with the aforementioned, the time series and 1:1 plots corresponding to ET_{ref} predictions based on the ASCE standardized PM equation showed a clear overestimation (Figs. 3.2, 3.3, 3.4, and 3.5). In contrast, ET_{ref} forecasts based on the HS equation demonstrated a superior fit (Figs. 3.6, 3.7, 3.8, and 3.9). This improvement is also evidenced in the statistical indicators, with 7-day average values for daily HS predictions in the ranges (excluding $Accuracy$, as it

was recently provided): $RMSE$: 0.59-0.98 $mm\,d^{-1}$; $NRMSE$: 16.1-24.1 %; MBE: 0.10-0.36 $1\,mm\,d^{-1}$; $NMBE$: 2.5-8.3 %; and R^2: 0.66-0.76.

The results obtained suggest effectiveness and potential of GFS meteorological forecasts as a basis for predicting near future ET, which could positively impact water management in agriculture, especially in irrigation scheduling. These findings could be relevant for farmers and researchers in Chile, as the topic of ET forecasting has not yet been widely developed in the country. Possibly, the implementation of local adjustments ET prediction process could improve the accuracy of forecasts and benefit irrigation management not only in Chile but also in other regions, given the global coverage of the GFS model. Finally, these considerations could guide future research in this field.

REFERENCES

Allen, R.G., 2005. The ASCE standardized reference evapotranspiration equation. Amer Society of Civil Engineers. Technical Committee on Standardization of Reference Evapotranspiration; Edited by Richard G. Allen, Ivan A. Walter, Ronald L. Elliott, Terry A. Howell, Daniel Itenfisu, Marvin E. Jensen, and Richard L. Snyder. ISBN (print): 9780784408056ISBN (PDF): 9780784475638. https://doi.org/10.1061/9780784408056.

Allen, R.G., Pereira, L.S., Raes, D., Smith, M., 1998. Crop evapotranspiration-guidelines for computing crop water requirements. FAO irrigation and drainage paper 56. Rome: Food and Agricultural Organization of the United Nations.

Chacon, G. (ed.), 2019. Descripcion y usos de la Red de Agrometeorologia INIA. Santiago, Chile: Boletin INIA - Instituto de Investigaciones Agropecuarias. no. 415. Available in: https://hdl.handle.net/20.500.14001/6836.

Chia, M.Y., Huang, Y.F., Koo, C.H., Fung, K.F., 2020. Recent Advances in Evapotranspiration Estimation Using Artificial Intelligence Approaches with a Focus on Hybridization Techniques—A Review. Agronomy, 10, 101. https://doi.org/10.3390/agronomy10010101

Fares, A., Abbas, F., 2009. Irrigation systems and nutrient sources for fertigation. Soil Crop Manage. 25 (May): 1–4.

Farooque, A.A., Afzaal, H., Abbas, F. et al., 2022. Forecasting daily evapotranspiration using artificial neural networks for sustainable irrigation scheduling. Irrig Sci 40, 55–69. https://doi.org/10.1007/s00271-021-00751-1.

Feng, K., Tian J. 2021. Forecasting reference evapotranspiration using data mining and limited climatic data, European Journal of Remote Sensing, 54:sup2, 363-371. https://doi.org/10.1080/22797254.2020.1801355.

GEE (Google Earth Engine). https://earthengine.google.com/ (Accessed June 6, 2022).

Granata F., Di Nunno F. 2021. Forecasting evapotranspiration in different climates using ensembles of recurrent neural networks. Agricultural Water Management, Volume 255, 107040. https://doi.org/10.1016/j.agwat.2021.107040.

Ha, W.S., Diak, R.G., Krajewski, R.W. Estimating Near Real-Time Hourly Evapotranspiration Using Numerical Weather Prediction Model Output and GOES Remote Sensing Data in Iowa. Remote Sens. 2020, 12, 2337. https://doi.org/10.3390/rs12142337.

Ben Hamouda, G., Zaccaria, D., Bali, K., Snyder, R.l., Ventura, F. 2022. Evaluation of Forecast Reference Evapotranspiration for Different Microclimate Regions in California to Enable Prospective Irrigation Scheduling. American Society of Civil Engineers. Volume 148, Issue 1. https://doi.org/10.1061/(ASCE)IR.1943-4774.0001632.

Hargreaves, G.H., Allen, R.G., 2003. History and evaluation of Hargreaves evapotranspiration equation J. Irrigat. Drain. Eng., 129, 53-63, doi:10.1061/(ASCE)0733-9437(2003)129:1(53)

Hargreaves, G.H., Samani, Z.A., 1985. Reference crop evapotranspiration from temperature. Appl. Eng. Agric. 1, 96–99

Moritz, S., Bartz-Beielstein T. 2017. imputeTS: Time Series Missing Value Imputation in R. The R Journal, 9(1), 207–218. doi:10.32614/RJ-2017-009.

Liu, B., M. Liu, Y. Cui, D. Shao, Z. Mao, L. Zhang, S. Khan, Y. Luo. 2020. Assessing forecasting performance of daily reference evapotranspiration using public weather forecast and numerical weather prediction. Journal of Hydrology, Volume 590, 125547. https://doi.org/10.1016/j.jhydrol.2020.125547.

Luo, Y., X. Chang, S. Peng, S. Khan, W. Wang, Q. Zheng, and X. Cai. 2014. Short-term forecasting of daily reference evapotranspiration using the Hargreaves-Samani model and temperature forecasts. Agric. Water Manage. 136 (Apr): 42–51. https://doi.org/10.1016/j.agwat.2014.01.006.

Luo, Y., Traore, S., Lyu, X. et al. 2015. Medium Range Daily Reference Evapotranspiration Forecasting by Using ANN and Public Weather Forecasts. Water Resour Manage 29, 3863–3876. https://doi.org/10.1007/s11269-015-1033-8.

Madramootoo, C. A., and J. Morrison. 2013. “Advances and challenges with micro-irrigation.” Irrig. Drain. 62 (3): 255–261. https://doi.org/10.1002/ird.1704.

NOAA/NCEP, The Global Forecast System (GFS). https://developers.google.com/earth-engine/datasets/catalog/NOAA_GFS0P25#description (Accessed June 6, 2022).

Perera K.C., A.W. Western, B. Nawarathna, B. George. 2014. Forecasting daily reference evapotranspiration for Australia using numerical weather prediction outputs. Agricultural and Forest Meteorology, Volume 194, Pages 50-63. https://doi.org/10.1016/j.agrformet.2014.03.014.

Piantadosi, J., Anderssen, R.S. and Boland J. (Eds). Forecasting daily reference evapotranspiration for Shepparton, Victoria, Australia using numerical weather prediction

outputs. 2013. MODSIM2013, 20th International Congress on Modelling and Simulation. https://doi.org/10.36334/modsim.2013.l16.perera.

Reichardt, K., Timm L.C. 2020. Soil, Plant and Atmosphere. Springer Nature Switzerland AG.

Rolph G., A. Stein, and B. Stunder.2017. Real-time Environmental Applications and Display sYstem: READY. Environmental Modelling and Software. Volume 95. Pages 210-228. https://doi.org/10.1016/j.envsoft.2017.06.025.

Santibanez, F. (2017) Atlas agroclimatico de Chile. Estado actual y tendencias del clima. Tomo III: Regiones de Valparaiso, Metropolitana, O'Higgins y Maule [online]. Santiago: Available in: https://hdl.handle.net/20.500.14001/62376.

Santibanez, F. (2017) Atlas agroclimatico de Chile. Estado actual y tendencias del clima. Tomo IV: Regiones del Biobio y la Araucania [online]. Santiago: Available in: https://hdl.handle.net/20.500.14001/62379.

Silva D., Meza F.J., Varas E. 2010. Estimating reference evapotranspiration (ETo) using numerical weather forecast data in Central Chile. Journal of Hydrology, Volume 382, Issues 1–4, Pages 64-71. https://doi.org/10.1016/j.jhydrol.2009.12.018.

Suryavanshi, P., G. S. Buttar, and A. S. Brar. 2015. "Micro irrigation for sustainable agriculture: A brief review." Indian J. Econ. Dev. 11 (1): 147–155. https://doi.org/10.5958/2322-0430.2015.00016.5.

Tian, D., and C. J. Martinez. 2012a. Forecasting Reference Evapotranspiration Using Retrospective Forecast Analogs in the Southeastern United States. J. Hydrometeor., 13, 1874–1892, https://doi.org/10.1175/JHM-D-12-037.1.

Tian, D., and C. J. Martinez. 2012b. Comparison of two analog-based downscaling methods for regional reference evapotranspiration forecasts. Journal of Hydrology. Volume 475. Pages 350-364. https://doi.org/10.1016/j.jhydrol.2012.10.009.

Traore, S., Y. Luo, and G. Fipps. 2016. Deployment of artificial neural network for short-term forecasting of evapotranspiration using public weather forecast restricted messages. Agric. Water Manage. 163 (Jan): 363–379. https://doi.org/10.1016/j.agwat.2015.10.009.

Van Doren, B.M., and Horton K.G. 2018. A continental system for forecasting bird migration.Science361,1115-1118.DOI:10.1126/science.aat7526

Wilks, D. S. 2005. Vol. 91 of Statistical methods in the atmospheric sciences. 2nd ed. New York: Academic Press.

Xue, M., J. Schleif, F. Kong, K. W. Thomas, Y. Wang, and K. Zhu. 2013. Track and Intensity Forecasting of Hurricanes: Impact of Convection-Permitting Resolution and Global Ensemble Kalman Filter Analysis on 2010 Atlantic Season Forecasts. Wea. Forecasting, 28, 1366–1384, https://doi.org/10.1175/WAF-D-12-00063.1.

Yang, Y., Y. Cui, Y. Luo, X. Lyu, S. Traore, S. Khan, and W. Wang. 2016. Short-term forecasting of daily reference evapotranspiration using the Penman-Monteith model and public weather forecasts. Agric. For. Meteorol. 177 (Nov): 329-339. https://doi.org/10.1016/j.agwat.2016.08.020.

Yang Y., Y Cui, K. Bai, T. Luo, J. Dai, W. Wang, Yufeng Luo. 2019a. Short-term forecasting of daily reference evapotranspiration using the reduced-set Penman-Monteith model and public weather forecasts. Agricultural Water Management. Volume 211. https://doi.org/10.1016/j.agwat.2018.09.036.

Yang Y., Y. Luo, C. Wu, H. Zheng, L. Zhang, Y. Cui, N. Sun, L. Wang. 2019b. Evaluation of six equations for daily reference evapotranspiration estimating using public weather forecast message for different climate regions across China. Agricultural Water Management. Volume 222. https://doi.org/10.1016/j.agwat.2019.06.014.

Yoo, H., Li, Z. 2012. Evaluation of cloud properties in the NOAA/NCEP global forecast system using multiple satellite products. Clim Dyn 39, 2769–2787. https://doi.org/10.1007/s00382-012-1430-0

Yue, H., M. Gebremichael, and V. Nourani. 2022. Evaluation of Global Forecast System (GFS) Medium-Range Precipitation Forecasts in the Nile River Basin. J. Hydrometeor., 23, 101–116, https://doi.org/10.1175/JHM-D-21-0110.1.

Zhang, L., X. Zhao, J. Ge, J. Zhang, S. Traore, G. Fipps, and Y. Luo. 2022. Evaluation of Five Equations for Short-Term Reference Evapotranspiration Forecasting Using Public Temperature Forecasts for North China Plain. Water 14, no. 18: 2888. https://doi.org/10.3390/w14182888.

Zhao J., Z. Guo, Z. Su, Z. Zhao, X. Xiao, and F. Liu. 2016. An improved multi-step forecasting model based on WRF ensembles and creative fuzzy systems for wind speed. Applied Energy. Volume 162. Pages 808-826. https://doi.org/10.1016/j.apenergy.2015.10.145.